Electronic Supplementary Information

Design and Synthesis of Yellow- to Red-Emitting Gold(III) Complexes Containing Isomeric Thienopyridine and Thienoquinoline Moieties and Their Applications in Operationally Stable Organic Light-Emitting Devices

Lok-Kwan Li,† Cathay Chai Au-Yeung,† Man-Chung Tang, Shiu-Lun Lai, Wai-Lung Cheung, Maggie Ng, Mei-Yee Chan, Vivian Wing-Wah Yam**

[*] Dr. L.-K. Li, Ms. C. C. A.-Y., Dr. M.-C. Tang, Dr. S.-L. Lai, Mr. W.-L. Cheung, Dr. M. Ng, Dr. M.-Y. Chan,* Prof. V. W.-W. Yam*
Institute of Molecular Functional Materials and Department of Chemistry, The University of Hong Kong, Pokfulam Road, Hong Kong (P. R. China)
Fax: +(852) 2857-1586; Tel: +(852) 2859-2153
E-mail: wwyam@hku.hk; chanmym@hku.hk

† L.-K.L. and C.C.A.Y. contributed equally to this work.

Table of Contents

Synthesis

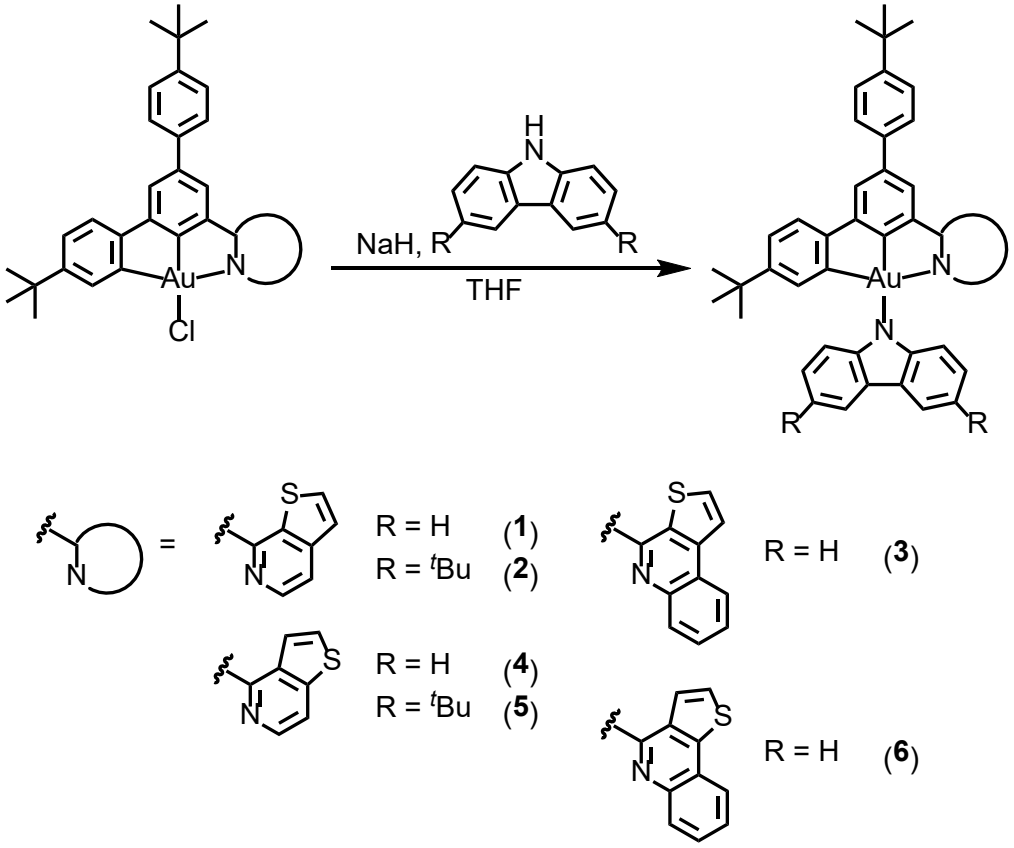

Scheme S1. Synthetic route for the carbazolylgold(III) complexes.

Thermogravimetric Analyses

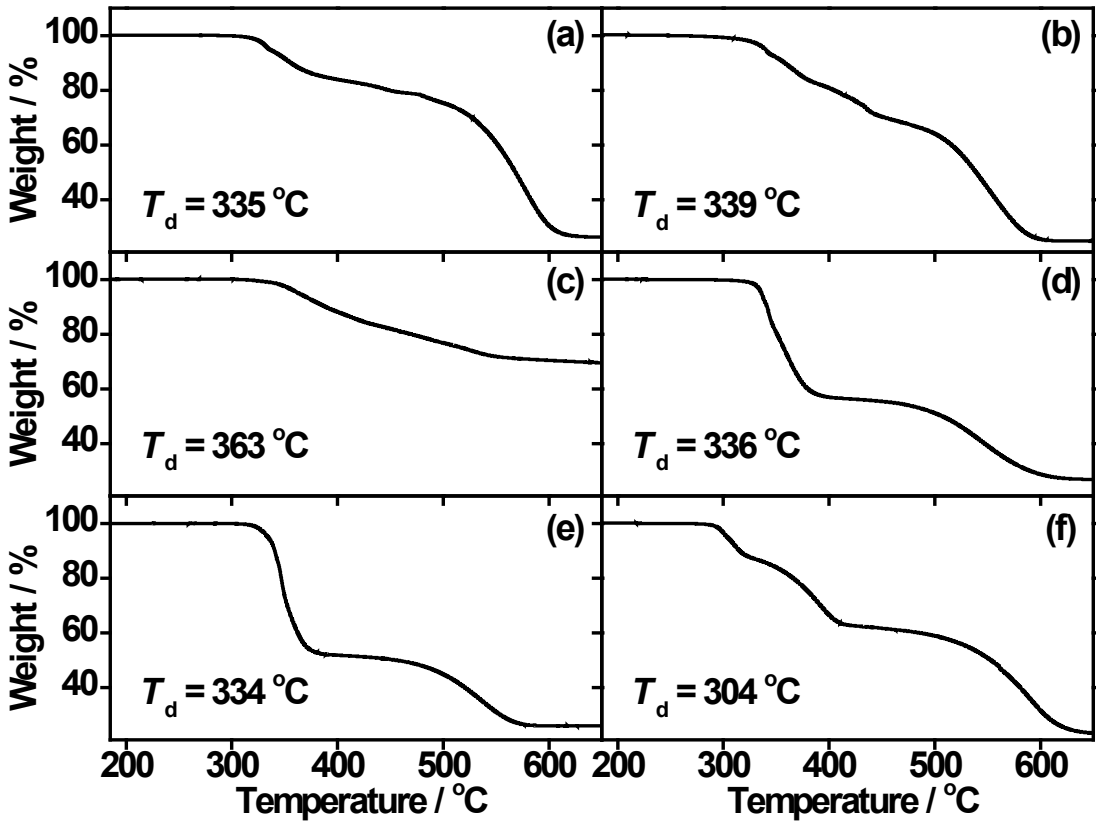

Figure S1. Thermogravimetric analysis (TGA) curves of (a) **1**, (b) **2**, (c) **3**, (d) **4**, (e) **5** and (f) **6**.

Table S1. Thermal properties of **1**−**6**.

Complex	T_d[a] / ºC
1	335
2	339
3	363
4	336
5	334
6	304

[a] T_d is defined as the decomposition temperature at which there is 5 wt% loss of the material.

Electrochemistry

Table S2. Electrochemical data of **1**−**6**.[a]

Complex	Oxidation $E_{1/2}^{ox}$ / V *vs.* SCE[b] (ΔE_p / mV)[c] [E_{pa} / V *vs.* SCE][d]	Reduction $E_{1/2}^{red}$ / V *vs.* SCE (ΔE_p / mV)	E_{HOMO}[e] / eV	E_{LUMO}[f] / eV
1	[+0.81], [+1.30]	−1.46 (73)	−5.15	−2.88
2	+0.67 (84)	−1.45 (85)	−5.01	−2.89
3	[+0.82], [+1.31]	−1.27 (57)	−5.16	−3.07
4	[+0.80], [+1.29]	−1.52 (87)	−5.14	−2.82
5	+0.66 (68)	−1.52 (82)	−5.00	−2.82
6	[+0.80], [+1.30]	−1.31 (86)	−5.14	−3.03

[a] In CH_2Cl_2 solution with 0.1 M $^nBu_4NPF_6$ as supporting electrolyte at 298 K; working electrode, glassy carbon; scan rate=100 mV s^{-1}.

[b] $E_{1/2} = (E_{pa} + E_{pc})/2$; E_{pa} and E_{pc} are the peak anodic and peak cathodic potentials, respectively.

[c] $\Delta E_p = (E_{pa} - E_{pc})$.

[d] E_{pa} refers to the anodic peak potential for the irreversible oxidation waves.

[e] E_{HOMO} levels are calculated from the electrode potentials, i.e. $E_{HOMO} = -[E_{pa}$ (*vs.* $Fc^+/Fc) + 4.80]$ eV or $E_{HOMO} = -[E_{1/2}^{ox}$ (*vs.* $Fc^+/Fc) + 4.80]$ eV. $E^o(Fc^+/Fc)$ = +0.46 V *vs.* SCE in CH_2Cl_2 (0.1 M $^nBu_4NPF_6$). From ref. 1.

[f] E_{LUMO} levels are calculated from the electrode potentials, i.e. $E_{LUMO} = -[E_{1/2}^{red}$ (*vs.* $Fc^+/Fc) + 4.80]$ eV. $E^o(Fc^+/Fc)$ = +0.46 V *vs.* SCE in CH_2Cl_2 (0.1 M $^nBu_4NPF_6$). From ref. 1.

Photophysical Properties

Table S3. Electronic absorption data of **1**−**6**.

Complex	Absorption λ_{max} / nm (ε / mol^{-1} dm^3 cm^{-1})
1	305 (24515), 337 (11270), 351 (13584), 365 (14190), 410 (2590)
2	308 (26940), 339 (10950), 356 (12580), 370 (12140), 410 (2450)
3	304 (26180), 331 (16920), 366 (19755), 388 (16420), 427 (2028)
4	305 (43670), 340 (20580), 366 (24180), 376 (20230), 409 (5160)
5	307 (38920), 341 (21320), 352 (20880), 366 (19170), 408 (4320)
6	304 (43770), 340 (20980), 365 (24445), 393 (19640), 430 (4340)

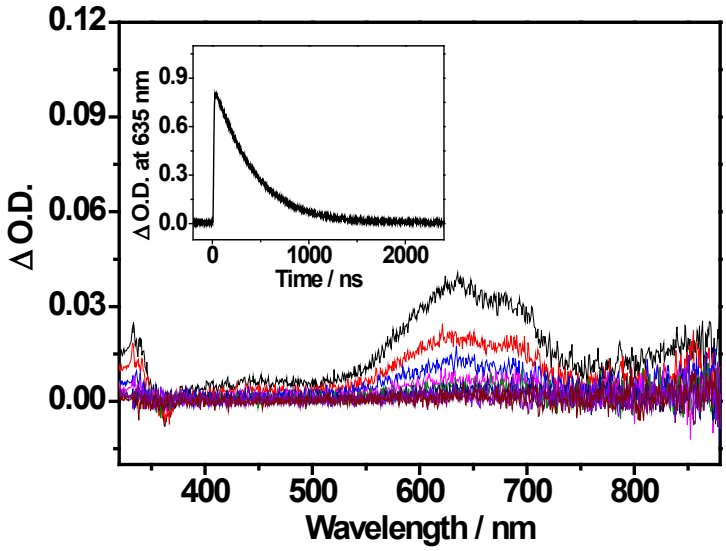

Figure S2. Transient absorption difference spectra of **1** in degassed toluene at 298 K at decay times of 0−1.6 μs with time intervals of 200 ns. Inset: The decay trace of the absorptions monitored at 635 nm.

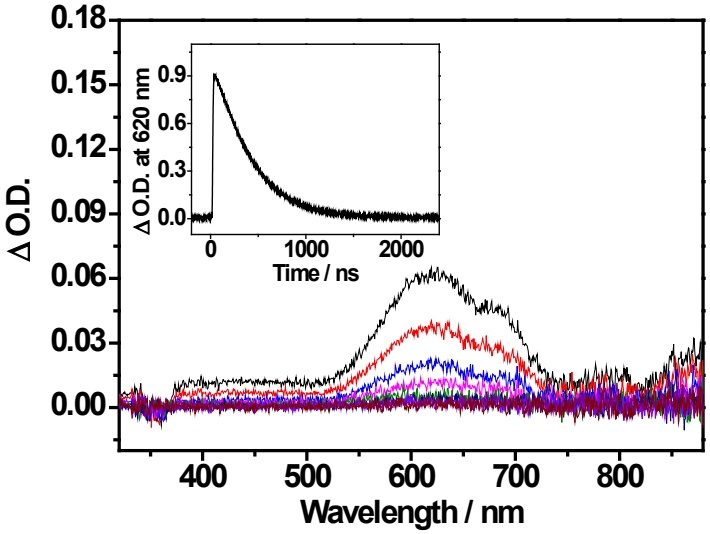

Figure S3. Transient absorption difference spectra of **4** in degassed toluene at 298 K at decay times of 0−1.6 μs with time intervals of 200 ns. Inset: The decay trace of the absorptions monitored at 620 nm.

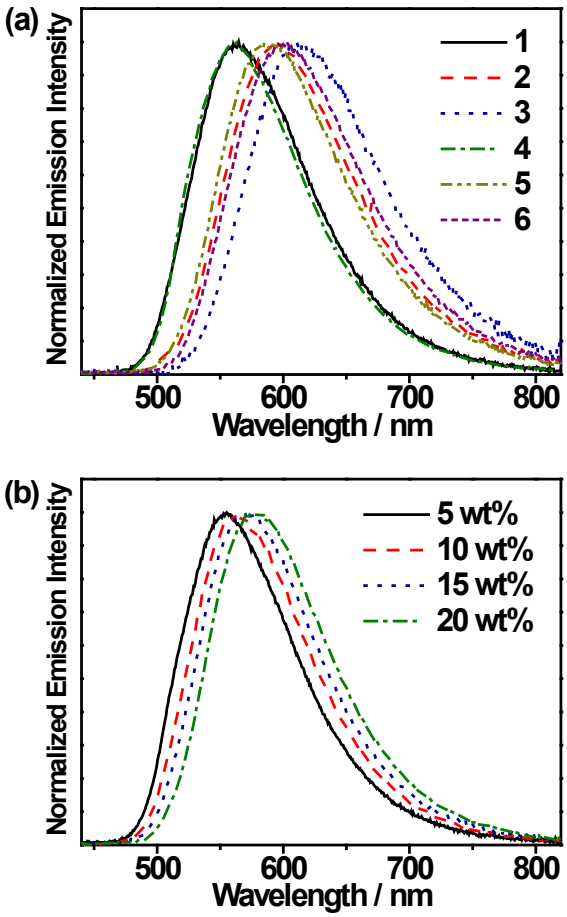

Figure S4. (a) Normalized PL spectra of **1**−**6** doped at 10 wt% in MCP thin films at 298 K. (b) Normalized PL spectra of **1** doped at 5−20 wt% in MCP thin films at 298 K.

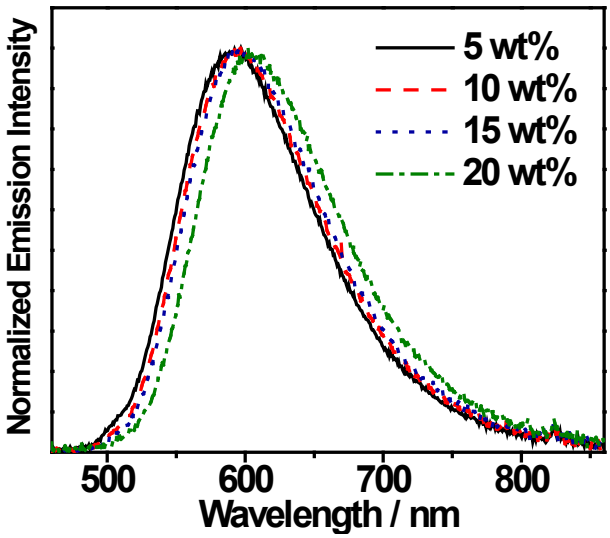

Figure S5. Normalized PL spectra of **2** doped at 5−20 wt% in MCP thin films at 298 K.

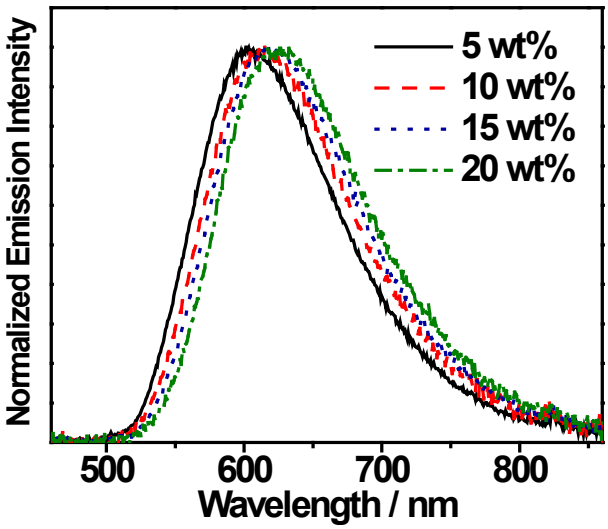

Figure S6. Normalized PL spectra of **3** doped at 5−20 wt% in MCP thin films at 298 K.

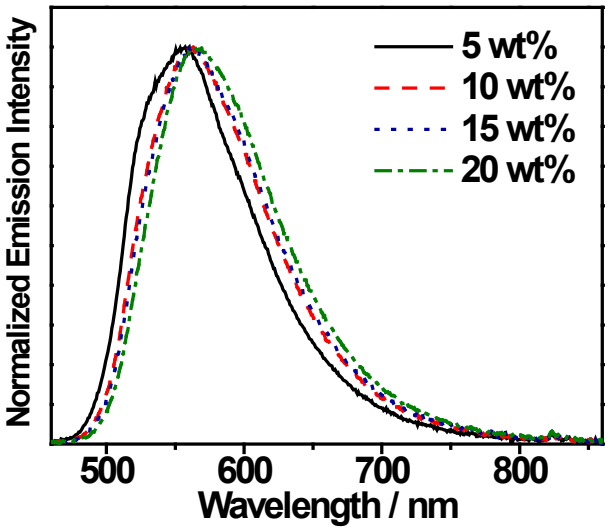

Figure S7. Normalized PL spectra of **4** doped at 5−20 wt% in MCP thin films at 298 K.

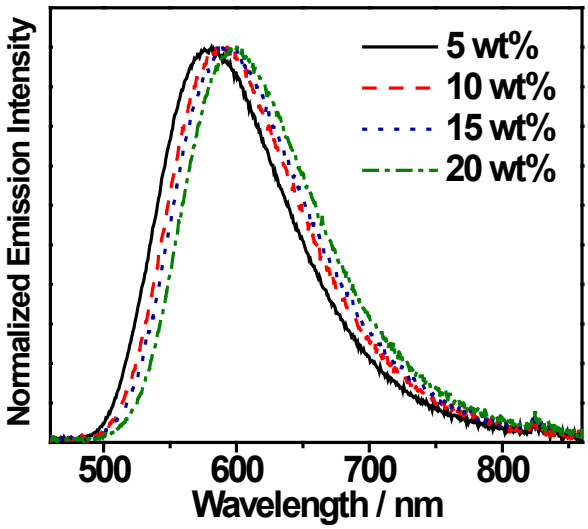

Figure S8. Normalized PL spectra of **5** doped at 5−20 wt% in MCP thin films at 298 K.

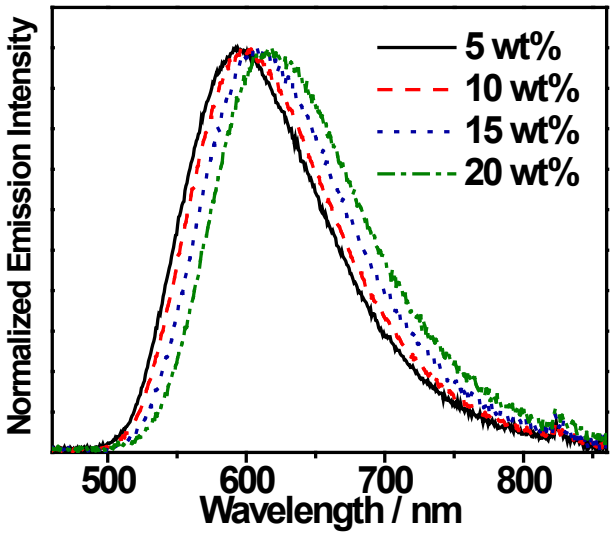

Figure S9. Normalized PL spectra of **6** doped at 5−20 wt% in MCP thin films at 298 K.

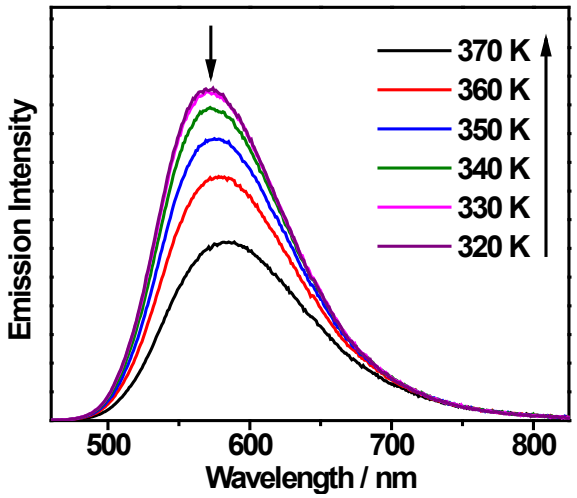

Figure S10. Emission spectra of the thin film of 20 wt% **1** doped in MCP upon increasing the temperature from 320 to 370 K.

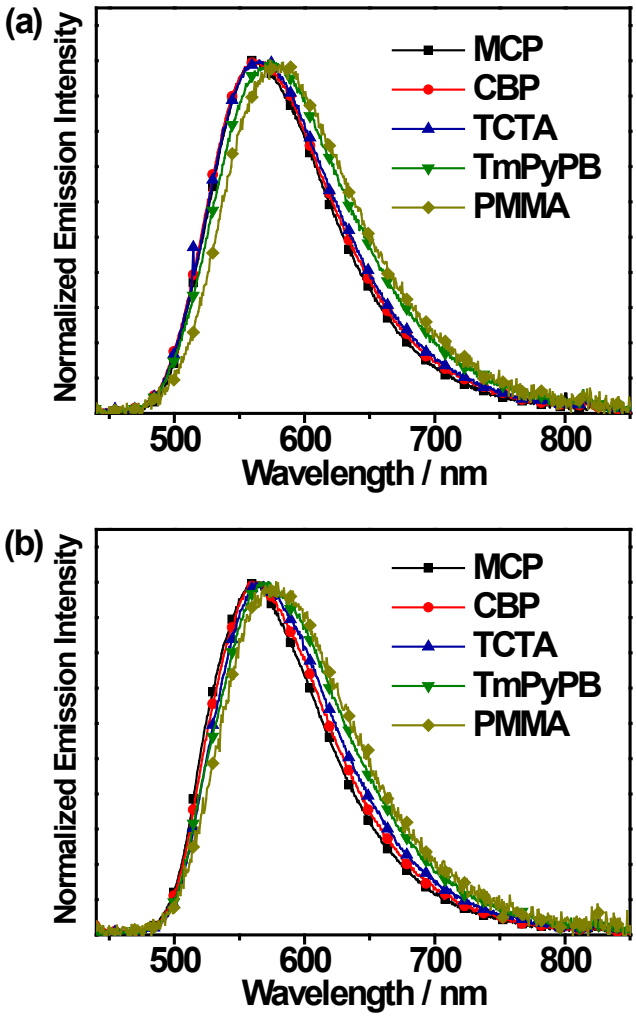

Figure S11. Normalized emission spectra of (a) **1** and (b) **4** doped in different host materials at 10 wt% at 298 K.

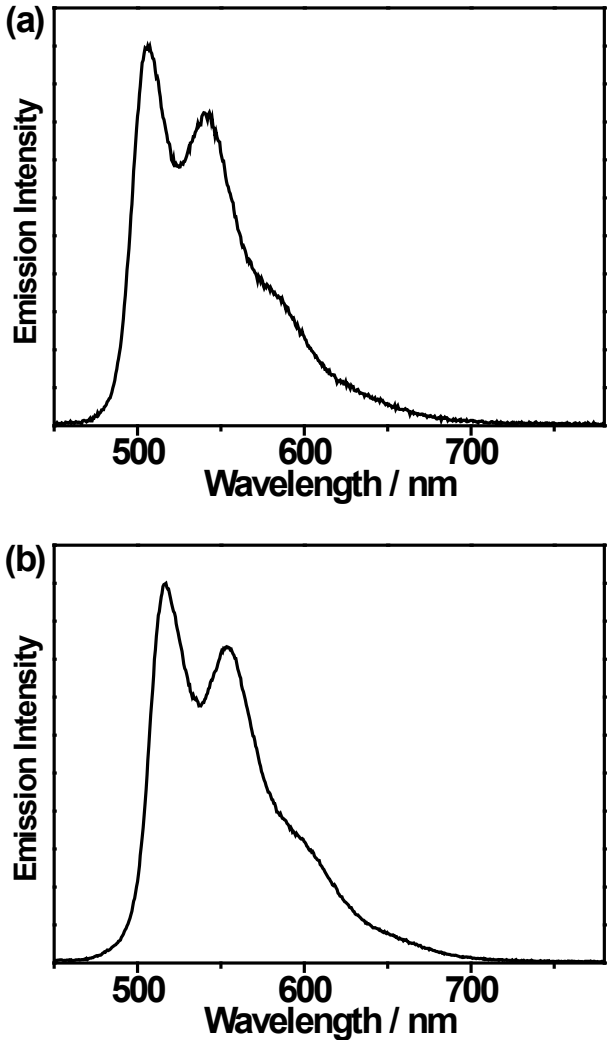

Figure S12. Emission spectra of [Au{4-^{t}BuC^C(4-^{t}BuC$_6$H$_4$)^N$_{(1\text{-thpy})}$}Cl] and [Au{4-^{t}BuC^C(4-^{t}BuC$_6$H$_4$)^N$_{(2\text{-thpy})}$}Cl] doped at 5 wt% in MCP at 298 K.

Computational Studies

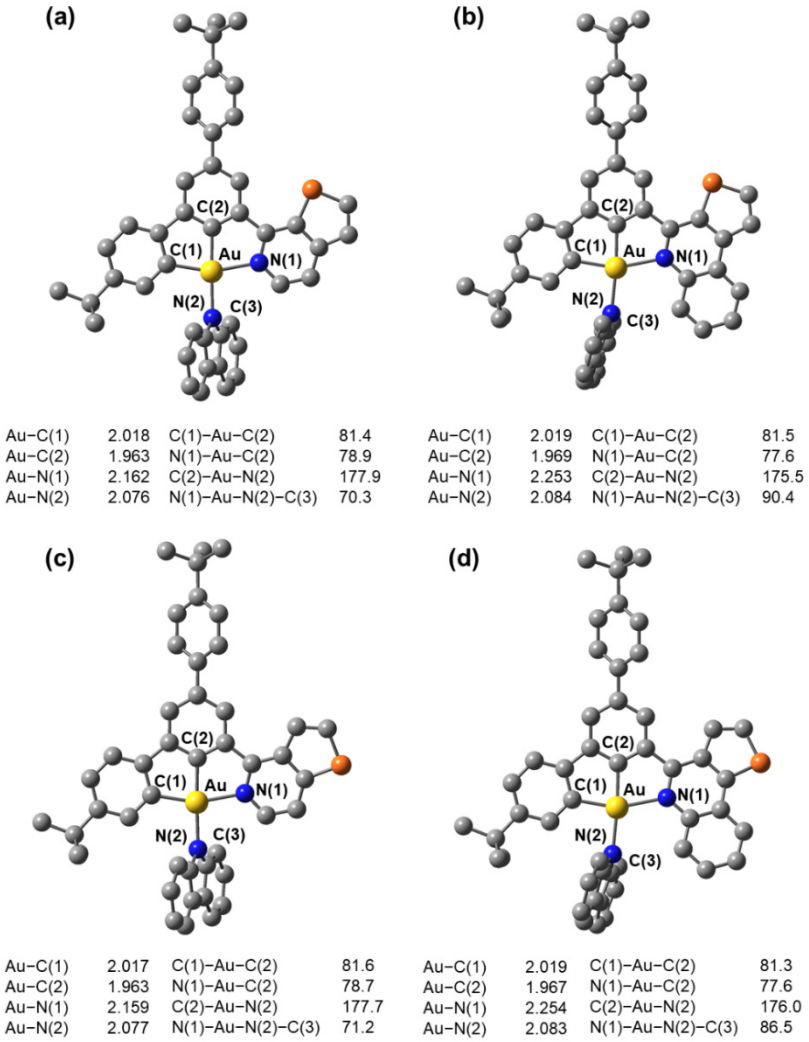

Au–C(1)	2.018	C(1)–Au–C(2)	81.4	Au–C(1)	2.019	C(1)–Au–C(2)	81.5
Au–C(2)	1.963	N(1)–Au–C(2)	78.9	Au–C(2)	1.969	N(1)–Au–C(2)	77.6
Au–N(1)	2.162	C(2)–Au–N(2)	177.9	Au–N(1)	2.253	C(2)–Au–N(2)	175.5
Au–N(2)	2.076	N(1)–Au–N(2)–C(3)	70.3	Au–N(2)	2.084	N(1)–Au–N(2)–C(3)	90.4

Au–C(1)	2.017	C(1)–Au–C(2)	81.6	Au–C(1)	2.019	C(1)–Au–C(2)	81.3
Au–C(2)	1.963	N(1)–Au–C(2)	78.7	Au–C(2)	1.967	N(1)–Au–C(2)	77.6
Au–N(1)	2.159	C(2)–Au–N(2)	177.7	Au–N(1)	2.254	C(2)–Au–N(2)	176.0
Au–N(2)	2.077	N(1)–Au–N(2)–C(3)	71.2	Au–N(2)	2.083	N(1)–Au–N(2)–C(3)	86.5

Figure S13. The optimized ground-state geometries (front view) with selected structural parameters of (a) **1**, (b) **3**, (c) **4** and (d) **6** at the PBE0 level of theory. The bond lengths and angles are in Angstroms and degrees, respectively. All hydrogen atoms are omitted for clarity.

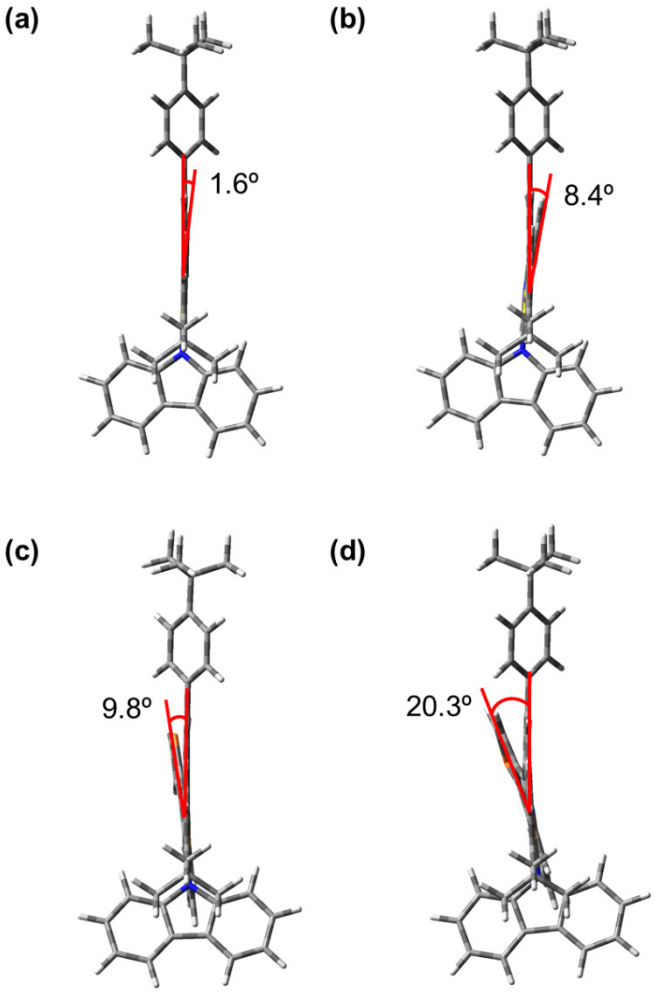

Figure S14. The optimized ground-state geometries (side view) of (a) **1**, (b) **3**, (c) **4** and (d) **6** at the PBE0 level of theory. The angle in red indicates the dihedral angle between the plane of the *N*-heterocycle and that of the central phenyl ring.

Table S4. The first fifteen singlet excited states (S_n) of **1**, **3**, **4** and **6** computed by TDDFT/CPCM using toluene as the solvent.

Complex	S_n	Excitation[a] (Coefficient)[b]	Vertical excitation wavelength / nm	f[c]	Character[d]
1	S_1	H→L (0.71)	565	0.005	LLCT
	S_2	H−1→L (0.71)	440	0.000	LLCT
	S_3	H−2→L (0.70)	400	0.067	ILCT/IL
	S_4	H→L+1 (0.70)	396	0.004	LLCT
	S_5	H→L+2 (0.70)	364	0.010	LLCT
	S_6	H→L+3 (0.67)	354	0.044	LLCT
	S_7	H−3→L (0.66)	349	0.096	IL/ILCT
	S_8	H−1→L+1 (0.70)	330	0.000	LLCT
	S_9	H→L+5 (0.58)	320	0.068	IL
		H→L+4 (−0.36)			LLCT
	S_{10}	H−4→L (0.51)	317	0.018	LLCT
		H−2→L+1 (0.41)			IL/ILCT
	S_{11}	H−4→L (0.48)	315	0.080	LLCT
		H−2→L+1 (−0.44)			IL/ILCT
	S_{12}	H−6→L (0.51)	308	0.090	IL/ILCT
		H−5→L (0.31)			ILCT/IL
	S_{13}	H−1→L+2 (0.66)	308	0.009	LLCT
	S_{14}	H→L+4 (0.58)	303	0.008	LLCT
		H→L+5 (0.34)			IL
	S_{15}	H−5→L (0.52)	302	0.168	ILCT/IL
		H−6→L (−0.41)			IL/ILCT
3	S_1	H→L (0.71)	596	0.000	LLCT
	S_2	H−1→L (0.71)	459	0.001	LLCT
	S_3	H−2→L (0.70)	421	0.046	ILCT/IL
	S_4	H→L+1 (0.69)	388	0.001	LLCT
	S_5	H→L+3 (0.66)	371	0.090	LLCT
	S_6	H−3→L (0.67)	367	0.159	IL/ILCT
	S_7	H→L+2 (0.68)	361	0.002	LLCT
	S_8	H−5→L (0.44)	338	0.098	IL/ILCT
		H−6→L (−0.43)			IL/ILCT
	S_9	H−4→L (0.62)	329	0.010	LLCT
	S_{10}	H−6→L (0.50)	327	0.175	IL/ILCT
		H−5→L (0.42)			IL/ILCT
	S_{11}	H−1→L+1 (0.70)	325	0.001	LLCT
	S_{12}	H→L+6 (0.62)	318	0.055	IL
	S_{13}	H−2→L+1 (0.54)	313	0.069	IL
		H−7→L (−0.37)			ILCT/IL
	S_{14}	H−1→L+2 (0.55)	308	0.001	LLCT
		H−1→L+3 (−0.43)			LLCT
	S_{15}	H−7→L (0.54)	308	0.119	ILCT/IL
		H−2→L+1 (0.34)			IL
4	S_1	H→L (0.70)	540	0.010	LLCT
	S_2	H−1→L (0.71)	424	0.000	LLCT

	S_3	H→L+1 (0.70)	418	0.002	LLCT
	S_4	H−2→L (0.70)	391	0.097	ILCT/IL
	S_5	H→L+2 (0.70)	367	0.006	LLCT
	S_6	H→L+3 (0.69)	350	0.035	LLCT
	S_7	H−1→L+1 (0.70)	346	0.001	LLCT
	S_8	H−3→L (0.67)	343	0.200	IL/ILCT
	S_9	H−2→L+1 (0.65)	322	0.073	ILCT/IL
	S_{10}	H→L+5 (0.67)	319	0.071	IL
	S_{11}	H−1→L+2 (0.70)	310	0.001	LLCT
	S_{12}	H−4→L (0.55)	309	0.060	LLCT
		H−5→L (−0.39)			IL/ILCT
	S_{13}	H−5→L (0.54)	307	0.025	IL/ILCT
		H−4→L (0.40)			LLCT
	S_{14}	H→L+4 (0.67)	303	0.003	LLCT
	S_{15}	H−6→L (0.66)	298	0.049	ILCT
6	S_1	H→L (0.71)	571	0.000	LLCT
	S_2	H−1→L (0.71)	443	0.001	LLCT
	S_3	H−2→L (0.69)	407	0.058	ILCT/IL
	S_4	H→L+1 (0.70)	406	0.005	LLCT
	S_5	H→L+2 (0.69)	386	0.002	LLCT
	S_6	H→L+3 (0.69)	368	0.057	LLCT
	S_7	H−3→L (0.67)	360	0.223	IL/ILCT
	S_8	H−1→L+1 (0.70)	340	0.000	LLCT
	S_9	H−5→L (0.55)	337	0.018	IL/ILCT
		H−4→L (0.32)			LLCT
	S_{10}	H−1→L+2 (0.69)	323	0.001	LLCT
	S_{11}	H−4→L (0.55)	321	0.007	LLCT
	S_{12}	H−6→L (0.34)	319	0.101	IL/ILCT
		H→L+5 (−0.33)			IL
		H−2→L+1 (−0.32)			ILCT/IL
	S_{13}	H→L+5 (0.59)	318	0.051	IL
	S_{14}	H−6→L (0.47)	314	0.126	IL/ILCT
		H−2→L+1 (0.44)			ILCT/IL
	S_{15}	H−2→L+2 (0.49)	307	0.003	IL
		H−2→L+3 (0.31)			IL

[a] Orbitals involved in the major excitation (H = HOMO and L = LUMO).

[b] The coefficients in the configuration interaction (CI) expansion that are less than 0.3 are not listed.

[c] Oscillator strengths.

[d] Character of the transition.

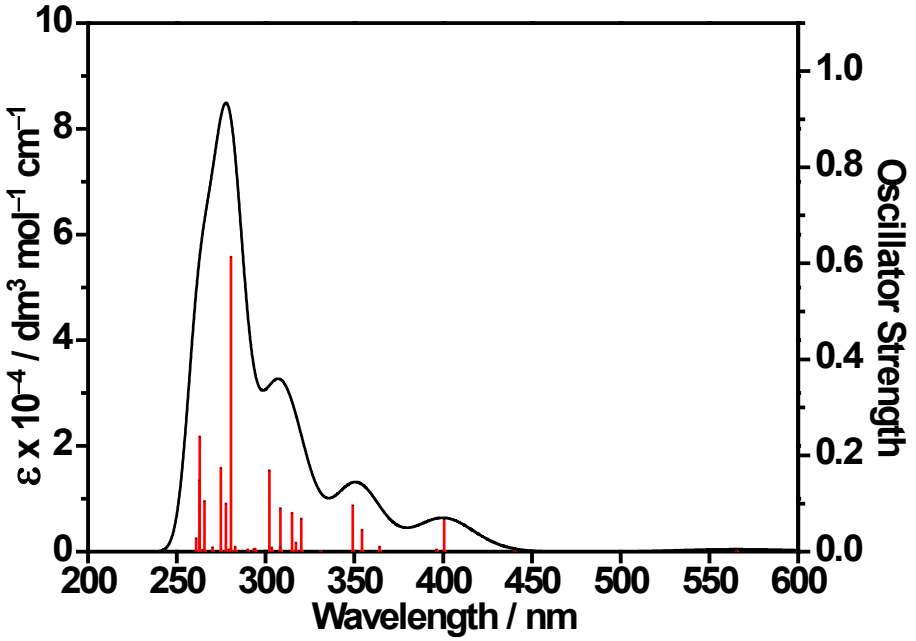

Figure S15. Simulated UV-vis spectrum of **1** computed by TDDFT/CPCM using toluene as the solvent.

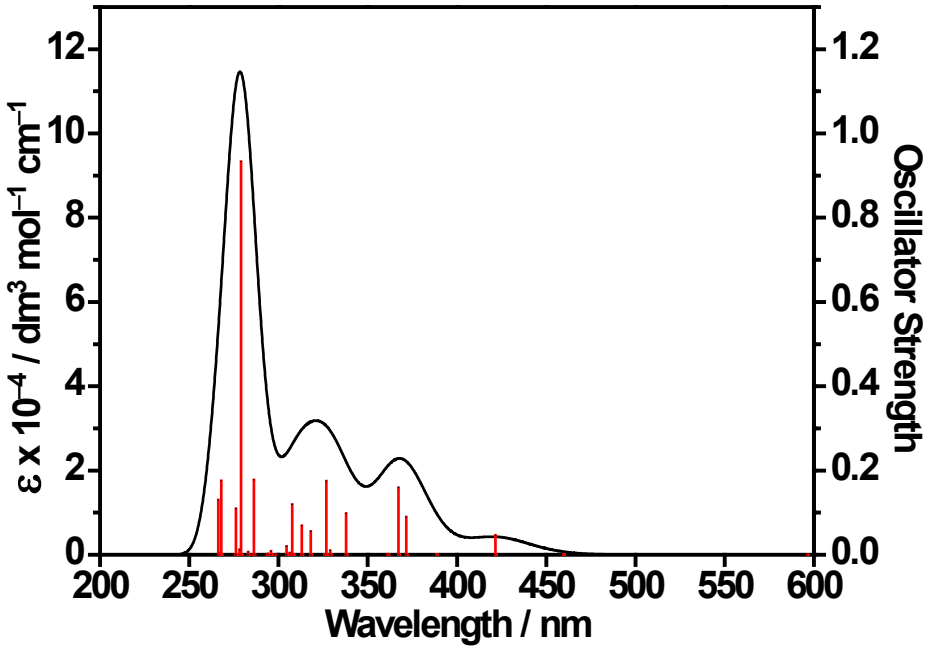

Figure S16. Simulated UV-vis spectrum of **3** computed by TDDFT/CPCM using toluene as the solvent.

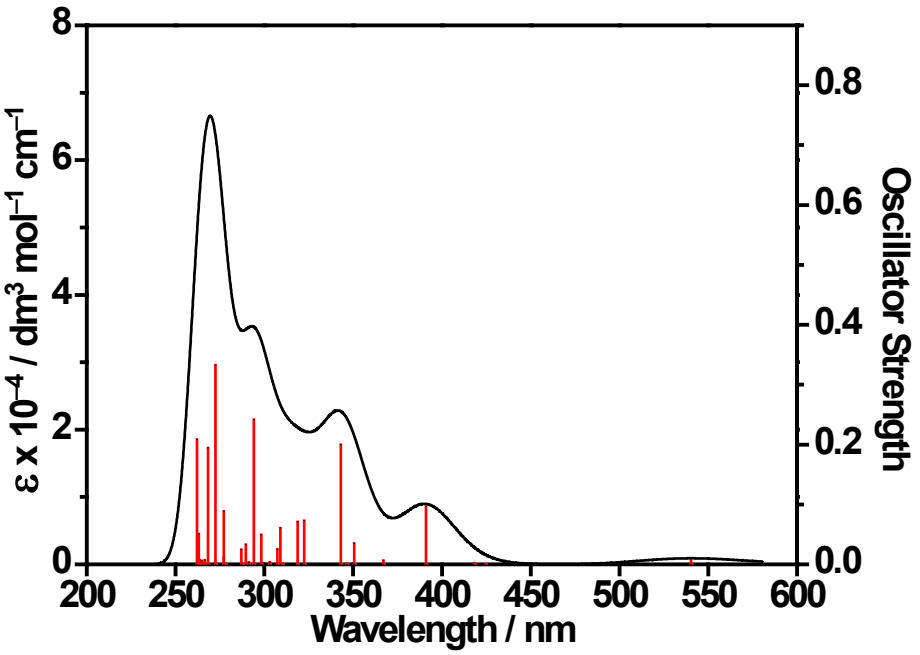

Figure S17. Simulated UV-vis spectrum of **4** computed by TDDFT/CPCM using toluene as the solvent.

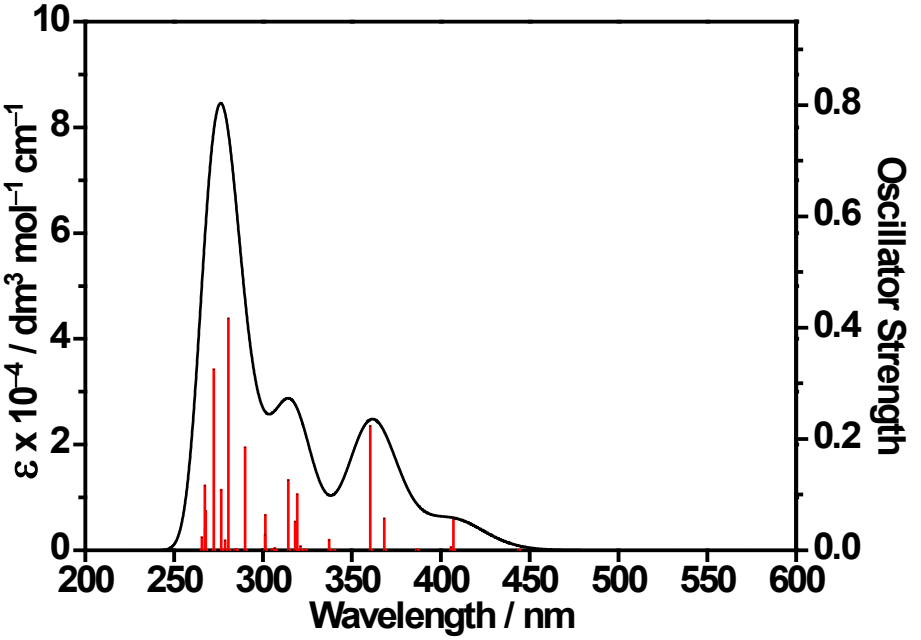

Figure S18. Simulated UV-vis spectrum of **6** computed by TDDFT/CPCM using toluene as the solvent.

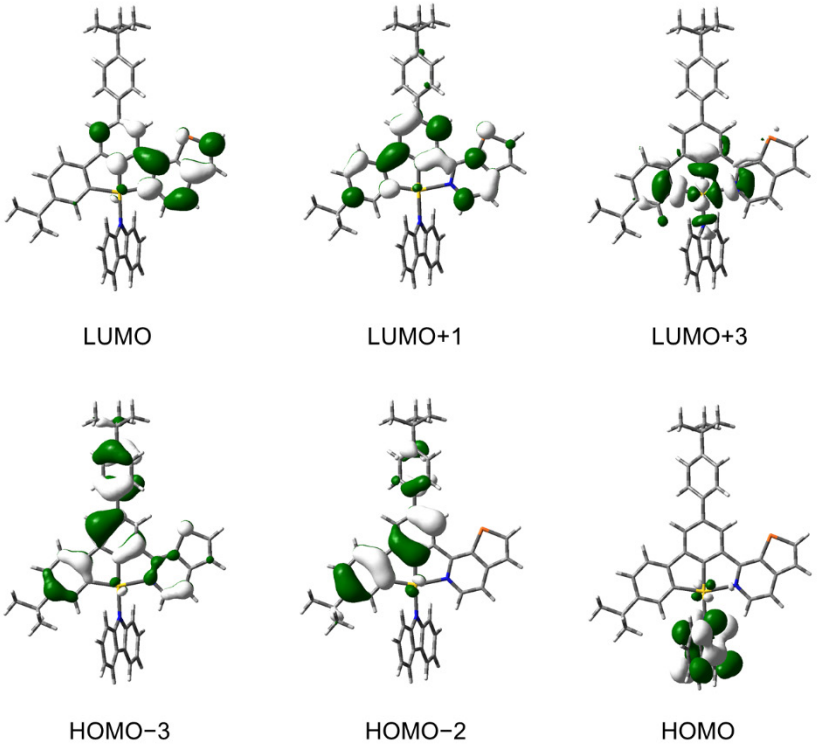

Figure S19. Spatial plots (isovalue = 0.03) of selected molecular orbitals of **1** at the optimized ground-state geometry.

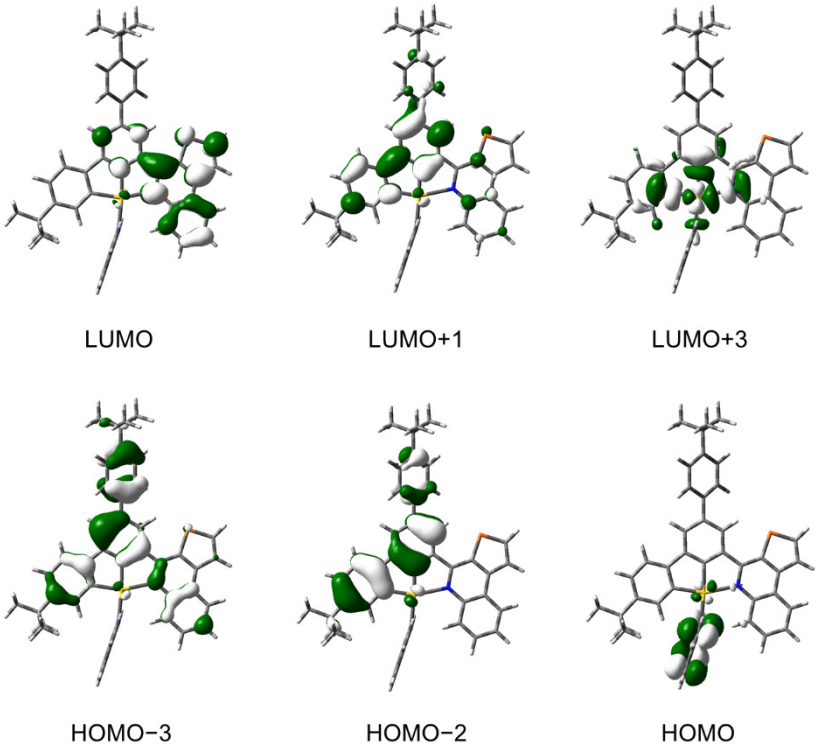

Figure S20. Spatial plots (isovalue = 0.03) of selected molecular orbitals of **3** at the optimized ground-state geometry.

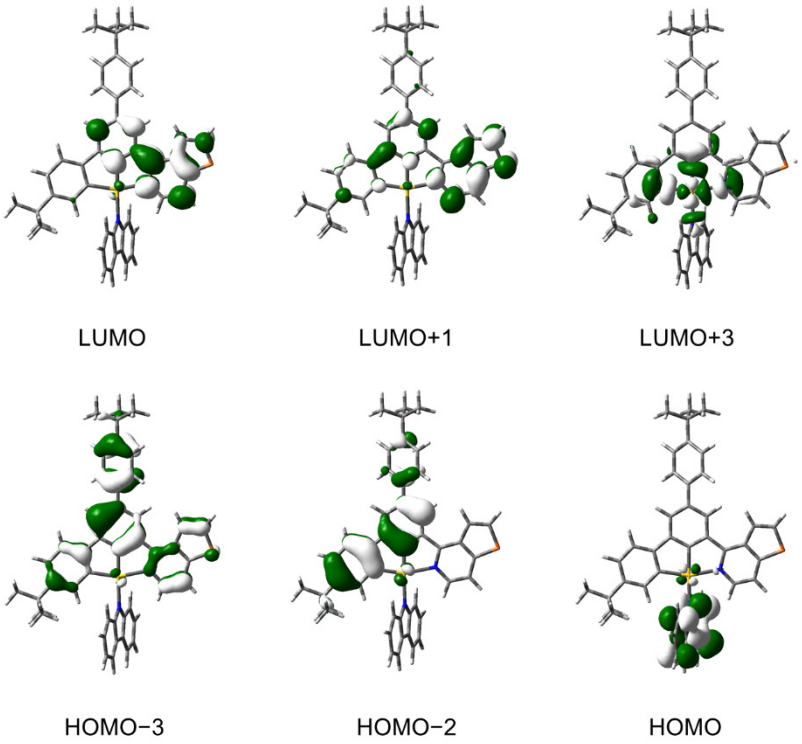

Figure S21. Spatial plots (isovalue = 0.03) of selected molecular orbitals of **4** at the optimized ground-state geometry.

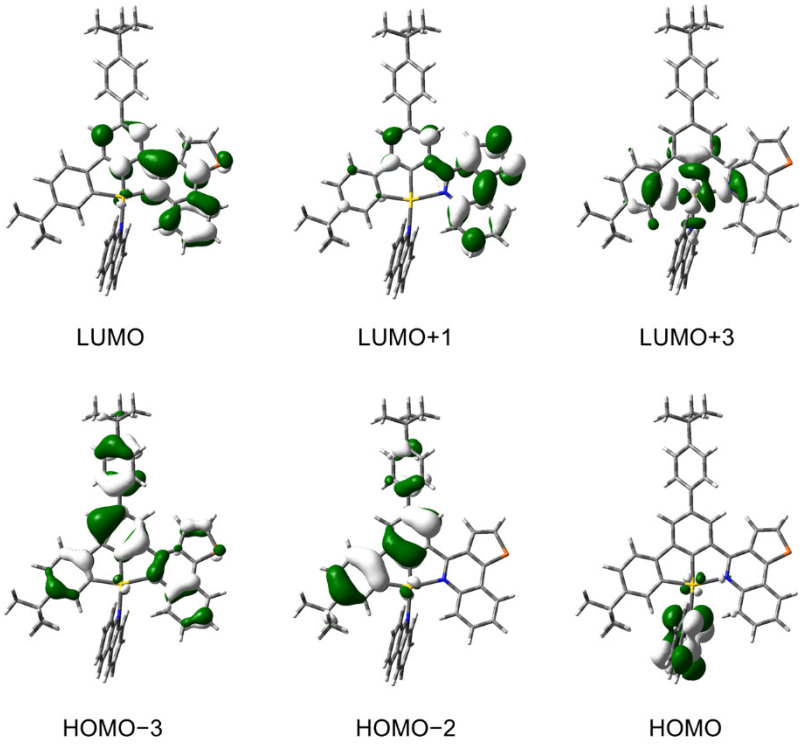

Figure S22. Spatial plots (isovalue = 0.03) of selected molecular orbitals of **6** at the optimized ground-state geometry.

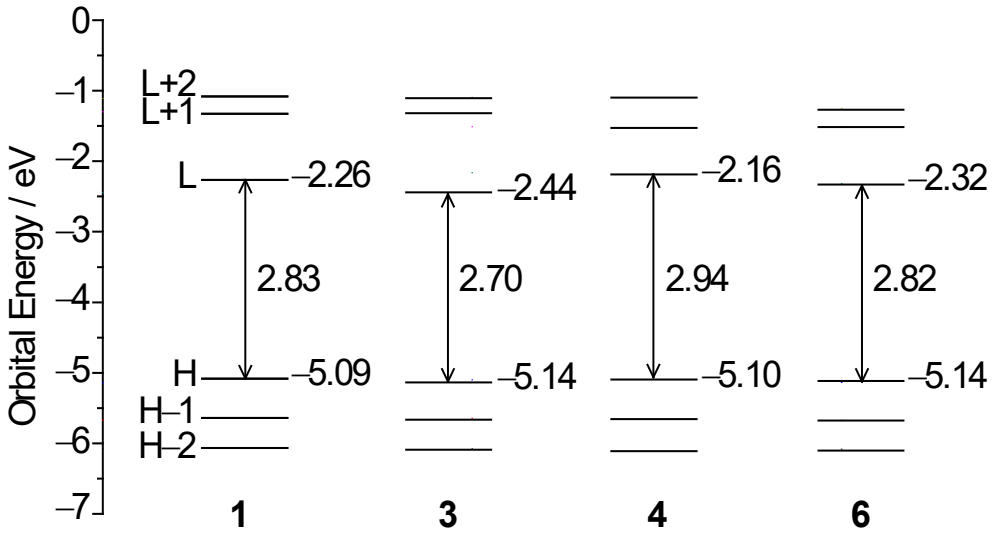

Figure S23. Orbital energy diagram of **1**, **3**, **4** and **6**.

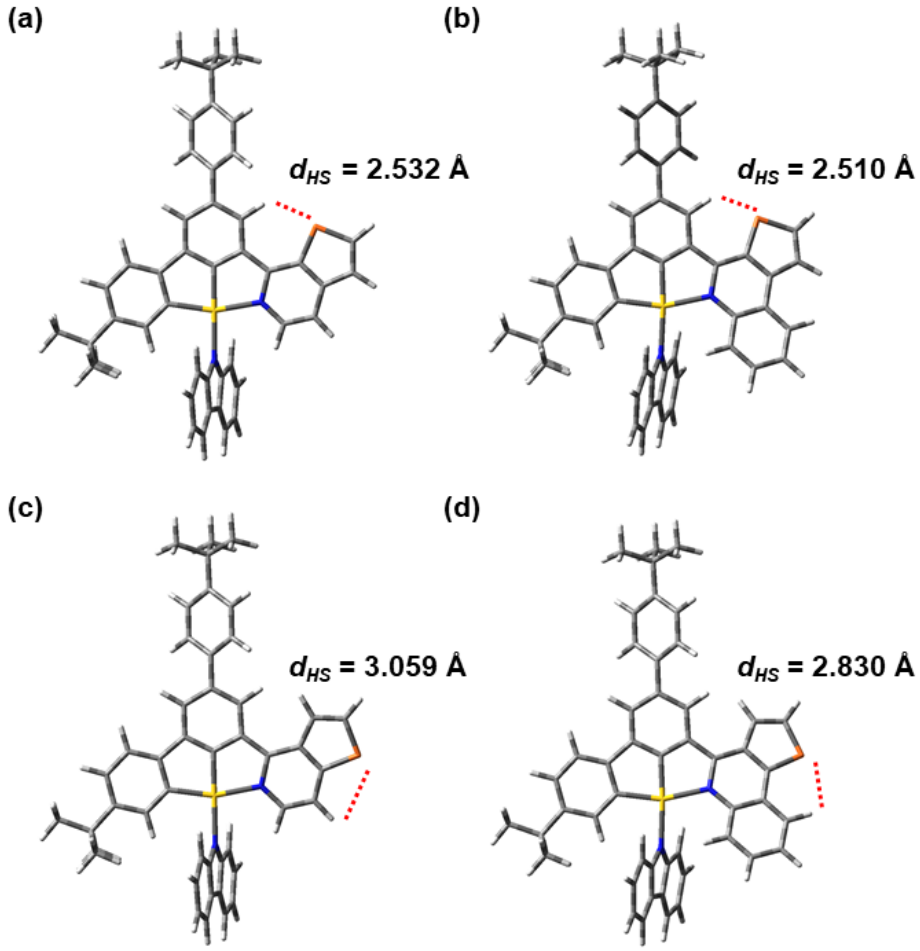

Figure S24. The distances between the sulfur and hydrogen atoms in the *N*-heterocyclic moieties of (a) **1**, (b) **3**, (c) **4** and (d) **6** at the optimized T_1 geometries.

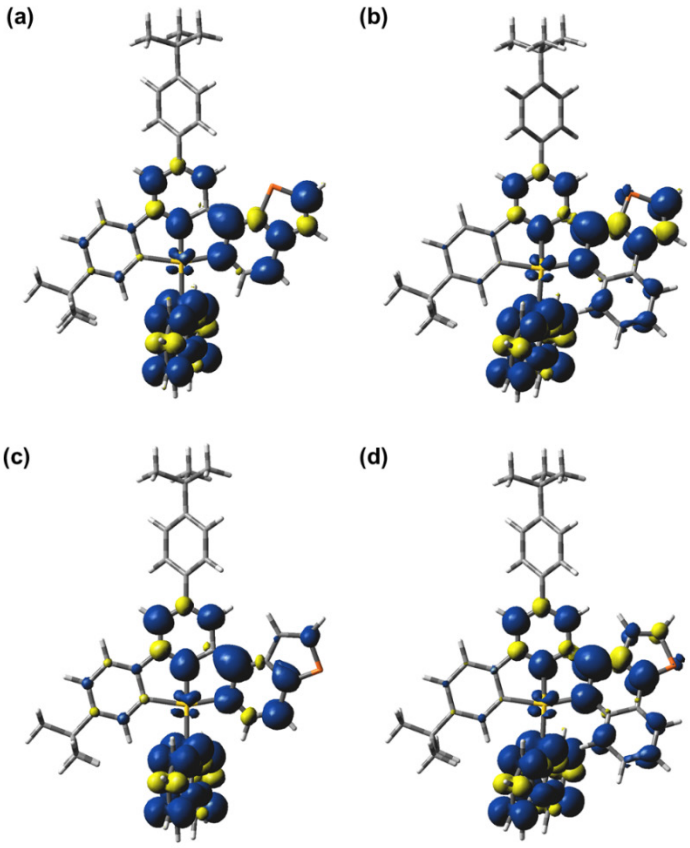

Figure S25. Plots of spin density (isovalue = 0.002) of the T_1 states of (a) **1**, (b) **3**, (c) **4** and (d) **6**.

Table S5. Relative energies of the optimized T_1 states of **1**, **3**, **4** and **6**.

Complex	$\Delta E(T_1–S_0)$ / cm^{-1} (λ / nm)[a]
1	17487 (572)
3	15830 (632)
4	17947 (557)
6	16353 (612)

[a] Energy difference between the T_1 and S_0 states at the corresponding optimized geometry in toluene.

Table S6. Cartesian coordinates of the optimized ground-state geometry of **1**.

1	C	-0.639759	0.033819	-0.027176
2	C	-2.860845	-0.852269	-0.059898
3	C	-3.366376	0.454239	-0.000291
4	C	-2.486009	1.549828	0.046930
5	C	-1.106930	1.347363	0.039484
6	H	-3.572544	-1.670279	-0.057402
7	H	-2.897372	2.555599	0.069157
8	C	-0.011356	2.327306	0.086180
9	C	-0.133535	3.711032	0.144490
10	C	1.293194	1.764766	0.067771
11	C	1.002092	4.522579	0.179922
12	H	-1.118133	4.172294	0.160725
13	C	2.410466	2.579107	0.105393
14	C	2.288986	3.982093	0.158649
15	H	0.865042	5.597665	0.222781
16	H	3.394481	2.120947	0.084421
17	C	-4.829830	0.676933	0.015713
18	C	-5.401416	1.681562	0.808359
19	C	-5.692668	-0.104788	-0.757996
20	C	-6.773703	1.887567	0.821337
21	H	-4.764555	2.292628	1.442462
22	C	-7.068948	0.105898	-0.739593
23	H	-5.283042	-0.874238	-1.407433
24	C	-7.644917	1.106054	0.048857
25	H	-7.173292	2.672427	1.458083
26	H	-7.693894	-0.522276	-1.365417
27	Au	1.302430	-0.251166	-0.020806
28	C	-9.151322	1.368668	0.093804
29	C	-9.933134	0.415796	-0.814289
30	H	-9.796791	-0.630314	-0.520253
31	H	-11.002244	0.641479	-0.747194
32	H	-9.638507	0.520061	-1.863874
33	C	-9.657340	1.185847	1.534348
34	H	-9.164443	1.872649	2.229040
35	H	-10.735014	1.377889	1.583371
36	H	-9.476855	0.164668	1.885770
37	C	-9.430150	2.809775	-0.364467
38	H	-8.929600	3.543538	0.274557
39	H	-9.085279	2.967178	-1.391662
40	H	-10.505805	3.015968	-0.330524
41	C	3.555092	4.840472	0.180235
42	C	4.357763	4.585895	-1.107113
43	H	5.279250	5.178901	-1.100292
44	H	4.637159	3.533302	-1.213965
45	H	3.776581	4.870504	-1.990629
46	C	3.239764	6.336313	0.263693
47	H	2.658293	6.678944	-0.598805
48	H	2.685182	6.585257	1.174783
49	H	4.174514	6.905954	0.278875
50	C	4.411088	4.459344	1.399603
51	H	3.862668	4.631459	2.331645
52	H	4.712235	3.407928	1.374563
53	H	5.322991	5.066346	1.423411
54	C	4.256901	-0.342138	-0.993115
55	C	4.049205	-1.180277	1.044442
56	C	4.033826	0.242398	-2.247312
57	C	5.569381	-0.726814	-0.597414
58	C	3.572202	-1.620560	2.287045
59	C	5.433998	-1.276055	0.726442
60	C	5.122205	0.434097	-3.087959
61	H	3.033058	0.540681	-2.549325
62	C	6.647636	-0.527716	-1.465340
63	C	4.480078	-2.159788	3.188811
64	H	2.518588	-1.532961	2.542128
65	C	6.327011	-1.823254	1.652601
66	C	6.420180	0.052502	-2.705982
67	H	4.965895	0.887795	-4.063132
68	H	7.652389	-0.821328	-1.170959
69	C	5.846672	-2.264913	2.878514
70	H	4.125753	-2.503485	4.157112
71	H	7.385664	-1.900399	1.416535
72	H	7.249206	0.214592	-3.388799
73	H	6.530601	-2.690507	3.607128
74	N	3.344238	-0.627620	-0.002191
75	C	-0.773223	-2.374617	-0.145059
76	C	-1.338985	-3.654624	-0.237626
77	C	-0.517415	-4.808987	-0.298800
78	C	1.375769	-3.370740	-0.181606
79	C	0.873769	-4.650384	-0.268345
80	C	-1.281110	-6.014971	-0.392237
81	C	-2.616132	-5.775522	-0.403971
82	H	2.441220	-3.167150	-0.155545
83	H	1.542224	-5.502592	-0.313440
84	H	-0.841834	-7.003495	-0.448399
85	H	-3.416935	-6.501299	-0.467769
86	C	-1.477204	-1.079979	-0.080395
87	S	-3.021557	-4.097978	-0.303095
88	N	0.582375	-2.287195	-0.120438

Table S7. Cartesian coordinates of the optimized ground-state geometry of **3**.

1	C	-0.779535	0.148314	0.042296
2	C	-3.023848	-0.674121	-0.014646
3	C	-3.502127	0.641770	0.023987
4	C	-2.595718	1.712878	0.082646
5	C	-1.223543	1.473556	0.082682
6	H	-3.754817	-1.466675	-0.118065
7	H	-2.979445	2.727986	0.140562
8	C	-0.120072	2.439875	0.126462
9	C	-0.225400	3.824954	0.194848
10	C	1.175185	1.865677	0.098306
11	C	0.919103	4.622630	0.235523
12	H	-1.204641	4.296865	0.218920
13	C	2.304082	2.662700	0.140678
14	C	2.198833	4.065823	0.209953
15	H	0.795210	5.698797	0.288821
16	H	3.283682	2.198142	0.117707
17	C	-4.959513	0.898053	-0.002666
18	C	-5.492666	1.977242	-0.720550
19	C	-5.854699	0.074604	0.686382
20	C	-6.859898	2.213638	-0.744558
21	H	-4.829489	2.624389	-1.288487
22	C	-7.225600	0.316694	0.657892
23	H	-5.474879	-0.754603	1.277872
24	C	-7.763536	1.390580	-0.057012
25	H	-7.229404	3.056462	-1.322745
26	H	-7.876901	-0.346575	1.217033
27	Au	1.165816	-0.150192	-0.015301
28	C	-9.263255	1.687185	-0.112969
29	C	-10.083127	0.686316	0.705518
30	H	-9.808495	0.705394	1.765493
31	H	-11.145791	0.939628	0.634686
32	H	-9.962093	-0.337606	0.336342
33	C	-9.525634	3.095971	0.444484
34	H	-8.998074	3.864789	-0.128079
35	H	-10.596355	3.325186	0.403392
36	H	-9.200892	3.170738	1.487454
37	C	-9.739689	1.621003	-1.573603
38	H	-9.217006	2.345989	-2.204827
39	H	-9.571325	0.624617	-1.995213
40	H	-10.811937	1.839210	-1.631673
41	C	3.477361	4.905097	0.250133
42	C	4.298633	4.640195	-1.023284
43	H	5.219607	5.233771	-1.006270
44	H	4.582328	3.587420	-1.115566
45	H	3.731805	4.916884	-1.918451
46	C	3.181179	6.405014	0.329698
47	H	2.615306	6.755137	-0.540214
48	H	2.618622	6.661778	1.233688
49	H	4.123279	6.961891	0.357068
50	C	4.307861	4.509384	1.482843
51	H	3.747285	4.689065	2.406220
52	H	4.593872	3.453458	1.461488
53	H	5.228037	5.103100	1.521805
54	C	4.028079	-0.046569	-1.184659
55	C	4.074946	-0.267775	1.017558
56	C	3.643267	0.038647	-2.528937
57	C	5.388811	0.132622	-0.807070
58	C	3.747021	-0.452895	2.366785
59	C	5.419219	-0.010904	0.626501
60	C	4.622122	0.298386	-3.478727
61	H	2.603201	-0.091496	-2.818083
62	C	6.356174	0.390018	-1.783847
63	C	4.765625	-0.381789	3.307639
64	H	2.719539	-0.643690	2.667275
65	C	6.427409	0.052813	1.593679
66	C	5.968446	0.472203	-3.114795
67	H	4.340404	0.369078	-4.525975
68	H	7.398250	0.525639	-1.504651
69	C	6.096011	-0.132464	2.929462
70	H	4.528321	-0.521717	4.358920
71	H	7.457331	0.246397	1.303770
72	H	6.709352	0.673127	-3.883186
73	H	6.869109	-0.083930	3.690851
74	N	3.243366	-0.304754	-0.081033
75	C	-0.988806	-2.261089	-0.006979
76	C	-1.662966	-3.507583	0.086889
77	C	-0.962664	-4.720669	0.035151
78	C	1.077520	-3.415918	-0.173392
79	C	-1.817485	-5.855475	0.166597
80	C	0.452034	-4.692201	-0.119207
81	C	2.480833	-3.352742	-0.312673
82	C	-3.119596	-5.500141	0.326019
83	H	-1.481154	-6.884306	0.151949
84	C	1.241822	-5.857602	-0.206554
85	H	2.953937	-2.376957	-0.348331
86	C	3.226399	-4.506652	-0.396524
87	H	-3.972819	-6.153933	0.453497
88	C	2.607891	-5.769413	-0.344109
89	H	0.761122	-6.829681	-0.166718
90	H	4.304404	-4.436815	-0.505317
91	H	3.207409	-6.671837	-0.412388
92	C	-1.646073	-0.940385	0.013513
93	S	-3.364838	-3.797348	0.319135
94	N	0.350857	-2.249117	-0.104993

Table S8. Cartesian coordinates of the optimized ground-state geometry of **4**.

1	C	-0.676292	0.063422	-0.098879
2	C	-2.890350	-0.830908	-0.071301
3	C	-3.401115	0.474020	-0.035059
4	C	-2.527451	1.575457	-0.040127
5	C	-1.148405	1.377142	-0.058288
6	H	-3.595532	-1.647704	0.006277
7	H	-2.943394	2.579584	-0.034996
8	C	-0.058372	2.364061	-0.034026
9	C	-0.189307	3.748245	-0.024762
10	C	1.249220	1.809199	-0.020995
11	C	0.941191	4.567480	-0.008132
12	H	-1.176642	4.203806	-0.034289
13	C	2.361387	2.631210	-0.002354
14	C	2.231360	4.034411	0.000348
15	H	0.797536	5.642559	-0.004495
16	H	3.348251	2.178716	0.002232
17	C	-4.864799	0.688558	0.019063
18	C	-5.420306	1.702003	0.812015
19	C	-5.744218	-0.109647	-0.718203
20	C	-6.793021	1.899409	0.861144
21	H	-4.769363	2.326964	1.417649
22	C	-7.120929	0.092257	-0.663713
23	H	-5.347233	-0.884244	-1.369467
24	C	-7.680752	1.100500	0.125987
25	H	-7.179601	2.691622	1.496808
26	H	-7.759382	-0.548619	-1.262458
27	Au	1.266281	-0.208200	-0.026213
28	C	-9.186960	1.354495	0.209917
29	C	-9.987995	0.383051	-0.660989
30	H	-9.836563	-0.657610	-0.355177
31	H	-11.056205	0.603153	-0.566785
32	H	-9.724161	0.473104	-1.720049
33	C	-9.650403	1.190585	1.666964
34	H	-9.142292	1.890870	2.336763
35	H	-10.727432	1.376860	1.743986
36	H	-9.453387	0.175996	2.028457
37	C	-9.488121	2.786694	-0.261939
38	H	-8.974566	3.533203	0.351478
39	H	-9.173570	2.930538	-1.300790
40	H	-10.563706	2.986725	-0.200547
41	C	3.492202	4.900746	0.003451
42	C	4.310560	4.603743	-1.264785
43	H	5.227939	5.203084	-1.270345
44	H	4.598348	3.549941	-1.328800
45	H	3.737268	4.850834	-2.164597
46	C	3.167484	6.396697	0.028003
47	H	2.593020	6.703539	-0.852489
48	H	2.602095	6.675910	0.923536
49	H	4.098765	6.972184	0.031538
50	C	4.336862	4.570142	1.245281
51	H	3.777258	4.773410	2.164311
52	H	4.643974	3.520295	1.262481
53	H	5.245074	5.183025	1.256411
54	C	4.251565	-0.334849	-0.891830
55	C	3.982209	-1.055194	1.183291
56	C	4.065928	0.173003	-2.184919
57	C	5.553448	-0.679652	-0.430120
58	C	3.467690	-1.428061	2.433036
59	C	5.378056	-1.152515	0.918291
60	C	5.180662	0.329188	-2.997958
61	H	3.073169	0.440648	-2.537836
62	C	6.658959	-0.517835	-1.271080
63	C	4.349868	-1.902198	3.394925
64	H	2.405280	-1.338868	2.647797
65	C	6.244549	-1.633565	1.904395
66	C	6.468524	-0.013338	-2.550474
67	H	5.053433	0.723523	-4.002716
68	H	7.655931	-0.781369	-0.926153
69	C	5.727258	-2.008391	3.137480
70	H	3.966152	-2.192960	4.369341
71	H	7.311362	-1.711317	1.708787
72	H	7.318964	0.119192	-3.213022
73	H	6.390228	-2.382128	3.912428
74	N	3.308014	-0.573328	0.082525
75	C	-0.791876	-2.351600	-0.176649
76	C	-1.354683	-3.637087	-0.345176
77	C	-0.479456	-4.753987	-0.309336
78	C	1.370710	-3.315550	-0.050460
79	C	0.896385	-4.605964	-0.150592
80	C	-2.833422	-5.399226	-0.687789
81	H	2.428943	-3.095925	0.045950
82	H	1.574996	-5.450261	-0.124198
83	H	-3.739139	-5.961996	-0.871673
84	C	-1.506426	-1.058182	-0.127301
85	N	0.556864	-2.246917	-0.061458
86	C	-2.711215	-4.053792	-0.580875
87	H	-3.556840	-3.394111	-0.702294
88	S	-1.331287	-6.244854	-0.518285

Table S9. Cartesian coordinates of the optimized ground-state geometry of **6**.

1	C	-0.809575	0.190917	0.129088
2	C	-3.040034	-0.664757	0.024180
3	C	-3.535506	0.645273	0.047837
4	C	-2.646480	1.728975	0.146383
5	C	-1.270859	1.509586	0.174799
6	H	-3.749742	-1.475139	-0.079878
7	H	-3.044361	2.740331	0.148555
8	C	-0.177157	2.487401	0.221955
9	C	-0.294483	3.870055	0.314402
10	C	1.123785	1.926221	0.176775
11	C	0.843213	4.677220	0.364152
12	H	-1.277828	4.332537	0.351605
13	C	2.245610	2.732067	0.230482
14	C	2.127937	4.132842	0.324827
15	H	0.709824	5.751163	0.436238
16	H	3.228653	2.275457	0.193779
17	C	-4.993929	0.886103	-0.037905
18	C	-5.606760	1.890967	0.722725
19	C	-5.809477	0.124137	-0.879431
20	C	-6.973833	2.115816	0.640822
21	H	-5.007868	2.487780	1.405631
22	C	-7.180653	0.354149	-0.956620
23	H	-5.365199	-0.643799	-1.507534
24	C	-7.798067	1.354300	-0.200092
25	H	-7.407171	2.900089	1.255879
26	H	-7.767666	-0.258517	-1.632535
27	Au	1.135545	-0.084721	-0.000729
28	C	-9.300324	1.637314	-0.259672
29	C	-10.027495	0.705630	-1.232820
30	H	-9.926043	-0.345559	-0.942820
31	H	-11.095668	0.945180	-1.239220
32	H	-9.657407	0.817811	-2.257390
33	C	-9.910251	1.445196	1.138814
34	H	-9.459126	2.117106	1.875213
35	H	-10.986065	1.651693	1.113479
36	H	-9.768815	0.417609	1.489507
37	C	-9.527228	3.087136	-0.718991
38	H	-9.064108	3.806881	-0.037243
39	H	-9.108163	3.251314	-1.717116
40	H	-10.599846	3.307499	-0.758974
41	C	3.398912	4.983011	0.372473
42	C	4.211464	4.751520	-0.913079
43	H	5.128246	5.351394	-0.891010
44	H	4.501565	3.703019	-1.030818
45	H	3.635012	5.043231	-1.797249
46	C	3.089766	6.478166	0.485291
47	H	2.514785	6.841100	-0.373300
48	H	2.531152	6.710897	1.398209
49	H	4.026950	7.042998	0.517751
50	C	4.243441	4.570013	1.589765
51	H	3.689138	4.724920	2.521380
52	H	4.539300	3.517633	1.543704
53	H	5.158326	5.171464	1.633444
54	C	3.962308	0.121539	-1.248385
55	C	4.075449	-0.323350	0.917161
56	C	3.536450	0.350019	-2.563417
57	C	5.338236	0.236143	-0.901575
58	C	3.788253	-0.639530	2.251466
59	C	5.411917	-0.053987	0.507831
60	C	4.489346	0.689298	-3.514501
61	H	2.485203	0.268432	-2.828886
62	C	6.278652	0.575919	-1.879446
63	C	4.838829	-0.686494	3.158088
64	H	2.767304	-0.840267	2.567487
65	C	6.452665	-0.110927	1.440172
66	C	5.850029	0.801872	-3.180895
67	H	4.175527	0.871999	-4.538826
68	H	7.331790	0.663920	-1.623614
69	C	6.161516	-0.426468	2.760780
70	H	4.633061	-0.929412	4.197204
71	H	7.476695	0.090871	1.135330
72	H	6.569781	1.068058	-3.949560
73	H	6.960311	-0.472496	3.495330
74	N	3.208251	-0.231583	-0.149958
75	C	-0.981063	-2.219859	0.096405
76	C	-1.636102	-3.464989	0.346076
77	C	-0.901140	-4.644942	0.177014
78	C	1.066614	-3.343703	-0.305225
79	C	0.464871	-4.628600	-0.192278
80	C	2.438530	-3.266050	-0.627273
81	C	-3.209336	-5.065534	0.948347
82	C	1.240139	-5.786782	-0.410189
83	H	2.896593	-2.285580	-0.703462
84	C	3.172540	-4.412113	-0.834359
85	H	-4.118015	-5.540181	1.293679
86	C	2.574032	-5.682039	-0.728021
87	H	0.771377	-6.763235	-0.324485
88	H	4.225607	-4.331387	-1.085561
89	H	3.164857	-6.576899	-0.896378
90	C	-1.659826	-0.910034	0.097857
91	N	0.338130	-2.188310	-0.142723
92	C	-2.967633	-3.737655	0.815361
93	H	-3.695508	-2.990932	1.096279
94	S	-1.847431	-6.045797	0.526848

Table S10. Cartesian coordinates of the optimized T_1 geometry of **1** computed by DFT/CPCM.

1	C	-0.649779	0.013854	-0.015925
2	C	-2.870397	-0.859426	-0.038869
3	C	-3.362855	0.447906	-0.005895
4	C	-2.480507	1.550026	0.023639
5	C	-1.104175	1.330901	0.023315
6	H	-3.586990	-1.673604	-0.019202
7	H	-2.883559	2.558721	0.018476
8	C	-0.008312	2.310617	0.054655
9	C	-0.135951	3.693744	0.087361
10	C	1.294450	1.741905	0.050774
11	C	0.995575	4.513276	0.114351
12	H	-1.123158	4.149770	0.091079
13	C	2.405092	2.571515	0.080159
14	C	2.282623	3.975779	0.110870
15	H	0.853358	5.588399	0.137975
16	H	3.398218	2.129855	0.078115
17	C	-4.825617	0.678635	0.003668
18	C	-5.393451	1.713386	0.760462
19	C	-5.696485	-0.123162	-0.741012
20	C	-6.764827	1.927546	0.769007
21	H	-4.751417	2.343100	1.370680
22	C	-7.071837	0.094379	-0.727005
23	H	-5.291183	-0.918006	-1.361658
24	C	-7.642139	1.124266	0.026565
25	H	-7.158855	2.736714	1.378764
26	H	-7.700691	-0.553260	-1.328932
27	Au	1.280590	-0.293964	-0.008243
28	C	-9.147442	1.395249	0.065965
29	C	-9.935695	0.417266	-0.809351
30	H	-9.803043	-0.619289	-0.481852
31	H	-11.003873	0.649828	-0.748220
32	H	-9.641548	0.485615	-1.862025
33	C	-9.651897	1.260920	1.512354
34	H	-9.152829	1.966496	2.183481
35	H	-10.728648	1.460016	1.558456
36	H	-9.475141	0.250493	1.895349
37	C	-9.422682	2.821823	-0.437428
38	H	-8.916606	3.573371	0.176114
39	H	-9.079771	2.944539	-1.470053
40	H	-10.497481	3.034114	-0.407234
41	C	3.546209	4.839377	0.135700
42	C	4.379702	4.559277	-1.126203
43	H	5.294469	5.162996	-1.118860
44	H	4.673656	3.507233	-1.194685
45	H	3.813832	4.809349	-2.029756
46	C	3.225405	6.336002	0.174117
47	H	2.656904	6.652505	-0.706666
48	H	2.653263	6.605941	1.067963
49	H	4.157448	6.910401	0.190947
50	C	4.378368	4.494921	1.382171
51	H	3.809363	4.690482	2.297009
52	H	4.679646	3.442905	1.392345
53	H	5.289307	5.103714	1.410261
54	C	4.240275	-0.449052	-1.059306
55	C	4.145763	-1.027708	1.077036
56	C	3.907312	-0.034921	-2.352895
57	C	5.581554	-0.744513	-0.688317
58	C	3.700075	-1.318266	2.370606
59	C	5.519232	-1.127349	0.718176
60	C	4.941075	0.078594	-3.280328
61	H	2.877461	0.190610	-2.612764
62	C	6.593272	-0.627672	-1.619816
63	C	4.651759	-1.715644	3.307611
64	H	2.648449	-1.233317	2.627493
65	C	6.448452	-1.522478	1.658929
66	C	6.259541	-0.212498	-2.921639
67	H	4.719211	0.397669	-4.293357
68	H	7.625400	-0.847524	-1.364152
69	C	6.000739	-1.816827	2.959430
70	H	4.340606	-1.948903	4.320541
71	H	7.502300	-1.607128	1.411551
72	H	7.046353	-0.115925	-3.663426
73	H	6.721736	-2.128912	3.708683
74	N	3.387409	-0.623853	0.003927
75	C	-0.794723	-2.383658	-0.088983
76	C	-1.335512	-3.683403	-0.148064
77	C	-0.523649	-4.836229	-0.181129
78	C	1.387091	-3.387563	-0.105623
79	C	0.895676	-4.659048	-0.156890
80	C	-1.279711	-6.037626	-0.241646
81	C	-2.628332	-5.824751	-0.256645
82	H	2.457487	-3.205285	-0.091844
83	H	1.569794	-5.507671	-0.184543
84	H	-0.831711	-7.024982	-0.273337
85	H	-3.426273	-6.553170	-0.298222
86	C	-1.481393	-1.122940	-0.052302
87	S	-3.019447	-4.134943	-0.197353
88	N	0.609422	-2.273892	-0.070434

Table S11. Cartesian coordinates of the optimized T_1 geometry of **3** computed by DFT/CPCM.

1	C	-0.813219	0.205539	-0.117515
2	C	-3.004389	-0.736841	-0.117002
3	C	-3.542548	0.552515	-0.051502
4	C	-2.695582	1.676706	0.003500
5	C	-1.312286	1.503990	-0.034054
6	H	-3.689326	-1.571840	-0.218346
7	H	-3.128124	2.667614	0.108983
8	C	-0.254467	2.517589	0.052619
9	C	-0.434784	3.891701	0.158003
10	C	1.066211	1.996808	0.044805
11	C	0.663210	4.748331	0.260378
12	H	-1.438495	4.309806	0.162466
13	C	2.143290	2.862291	0.154631
14	C	1.968274	4.256846	0.264132
15	H	0.480731	5.814522	0.341091
16	H	3.152847	2.463260	0.156540
17	C	-5.011790	0.735353	-0.040384
18	C	-5.615707	1.809237	-0.709148
19	C	-5.851510	-0.152724	0.638952
20	C	-6.993217	1.979158	-0.695723
21	H	-4.997345	2.506471	-1.268311
22	C	-7.233002	0.021217	0.647410
23	H	-5.417288	-0.982227	1.190997
24	C	-7.839834	1.090336	-0.017878
25	H	-7.416527	2.821835	-1.236507
26	H	-7.837639	-0.693072	1.196313
27	Au	1.132038	-0.039129	-0.134816
28	C	-9.353238	1.314657	-0.030443
29	C	-10.104616	0.245030	0.766632
30	H	-9.806256	0.238442	1.820323
31	H	-11.179918	0.447560	0.728243
32	H	-9.941604	-0.757280	0.356654
33	C	-9.670924	2.686914	0.586140
34	H	-9.192369	3.501019	0.033383
35	H	-10.752063	2.866074	0.575756
36	H	-9.326885	2.737740	1.624414
37	C	-9.861019	1.279523	-1.481485
38	H	-9.389029	2.052434	-2.095596
39	H	-9.653646	0.309208	-1.944472
40	H	-10.943895	1.446044	-1.508285
41	C	3.199134	5.159716	0.377020
42	C	4.070449	4.992598	-0.879447
43	H	4.961730	5.626672	-0.809817
44	H	4.404887	3.958523	-1.009288
45	H	3.516415	5.281774	-1.778668
46	C	2.822862	6.638296	0.505416
47	H	2.265687	6.993489	-0.367822
48	H	2.219097	6.827616	1.399184
49	H	3.732584	7.242247	0.585638
50	C	4.014980	4.762584	1.618677
51	H	3.418476	4.875200	2.529935
52	H	4.357029	3.724322	1.566888
53	H	4.900812	5.401406	1.709730
54	C	4.184826	0.235348	-0.911365
55	C	3.947556	-0.544246	1.150009
56	C	3.935715	0.703763	-2.204611
57	C	5.505466	0.113422	-0.399171
58	C	3.415353	-1.019771	2.352921
59	C	5.349754	-0.399685	0.957541
60	C	5.034457	1.053835	-2.987116
61	H	2.919204	0.793324	-2.575568
62	C	6.583099	0.464451	-1.188270
63	C	4.309137	-1.351646	3.368406
64	H	2.342511	-1.125623	2.481785
65	C	6.221393	-0.733057	1.974625
66	C	6.334462	0.936840	-2.488650
67	H	4.878023	1.422133	-3.995661
68	H	7.602085	0.381606	-0.822604
69	C	5.686860	-1.211360	3.184022
70	H	3.930117	-1.724982	4.314007
71	H	7.295774	-0.632723	1.854035
72	H	7.173009	1.216558	-3.118904
73	H	6.361713	-1.477642	3.991638
74	N	3.256972	-0.163709	0.024491
75	C	-0.884422	-2.193447	-0.163691
76	C	-1.411598	-3.480065	0.049300
77	C	-0.616912	-4.636448	-0.006746
78	C	1.271947	-3.181316	-0.591794
79	C	-1.345549	-5.819210	0.295230
80	C	0.767434	-4.499803	-0.388983
81	C	2.593233	-3.052382	-1.059135
82	C	-2.659078	-5.582436	0.574763
83	H	-0.915968	-6.814369	0.305217
84	C	1.613717	-5.599703	-0.587298
85	H	2.962857	-2.064110	-1.299692
86	C	3.410537	-4.156590	-1.248864
87	H	-3.430940	-6.296147	0.828048
88	C	2.929221	-5.442474	-0.999980
89	H	1.220686	-6.598514	-0.420205
90	H	4.425317	-4.011371	-1.609326
91	H	3.564778	-6.310349	-1.146715
92	C	-1.608859	-0.948491	-0.130337
93	S	-3.053414	-3.896511	0.482247
94	N	0.493083	-2.063241	-0.371373

Table S12. Cartesian coordinates of the optimized T_1 geometry of **4** computed by DFT/CPCM.

1	C	-0.687011	0.045430	-0.067107
2	C	-2.902671	-0.837214	-0.048191
3	C	-3.399878	0.466478	-0.039459
4	C	-2.525081	1.576930	-0.049332
5	C	-1.148086	1.360148	-0.047478
6	H	-3.616059	-1.647312	0.039796
7	H	-2.933110	2.583061	-0.077030
8	C	-0.058751	2.347833	-0.023866
9	C	-0.196051	3.730287	-0.025265
10	C	1.247574	1.789163	0.004851
11	C	0.929711	4.558452	-0.002474
12	H	-1.186267	4.179264	-0.045657
13	C	2.352323	2.626395	0.030191
14	C	2.220104	4.030394	0.024537
15	H	0.779804	5.632819	-0.006945
16	H	3.348287	2.191731	0.053484
17	C	-4.863531	0.688455	-0.002431
18	C	-5.422557	1.731334	0.750049
19	C	-5.745294	-0.129209	-0.716537
20	C	-6.794937	1.936273	0.785391
21	H	-4.771176	2.375004	1.335285
22	C	-7.121712	0.078600	-0.675710
23	H	-5.346761	-0.928197	-1.336388
24	C	-7.682766	1.115652	0.074924
25	H	-7.181311	2.752390	1.390851
26	H	-7.759045	-0.581489	-1.254863
27	Au	1.244997	-0.247506	-0.008665
28	C	-9.188724	1.377271	0.142972
29	C	-9.989086	0.380506	-0.699568
30	H	-9.841890	-0.649944	-0.359192
31	H	-11.057304	0.606687	-0.618419
32	H	-9.718708	0.434534	-1.759432
33	C	-9.660715	1.262341	1.601931
34	H	-9.151630	1.981304	2.250943
35	H	-10.737466	1.455524	1.668627
36	H	-9.469109	0.259100	1.996549
37	C	-9.484855	2.793895	-0.376378
38	H	-8.970789	3.558231	0.214272
39	H	-9.165224	2.902708	-1.417989
40	H	-10.560195	2.999576	-0.326107
41	C	3.477497	4.903077	0.044995
42	C	4.330381	4.597295	-1.197857
43	H	5.240970	5.207360	-1.193207
44	H	4.632171	3.545919	-1.235853
45	H	3.775437	4.820661	-2.115088
46	C	3.146385	6.397944	0.041264
47	H	2.587871	6.688186	-0.854828
48	H	2.560194	6.686242	0.920149
49	H	4.074280	6.979106	0.056218
50	C	4.294588	4.595885	1.311001
51	H	3.711705	4.810626	2.212715
52	H	4.602282	3.546476	1.351883
53	H	5.201202	5.211263	1.336175
54	C	4.225954	-0.403453	-1.002663
55	C	4.101925	-0.929576	1.145257
56	C	3.910543	-0.025277	-2.311595
57	C	5.563993	-0.674497	-0.602535
58	C	3.638245	-1.192290	2.438598
59	C	5.482349	-1.022943	0.811721
60	C	4.958455	0.076698	-3.224384
61	H	2.882864	0.182450	-2.593929
62	C	6.589979	-0.569742	-1.519951
63	C	4.578364	-1.555595	3.400734
64	H	2.581849	-1.111227	2.676471
65	C	6.399964	-1.384016	1.777366
66	C	6.273813	-0.190792	-2.836995
67	H	4.750172	0.368150	-4.248574
68	H	7.619950	-0.771853	-1.241862
69	C	5.933990	-1.650682	3.077301
70	H	4.253012	-1.766351	4.414152
71	H	7.458665	-1.462862	1.549530
72	H	7.071837	-0.103952	-3.567932
73	H	6.645746	-1.935721	3.845921
74	N	3.356900	-0.561647	0.050182
75	C	-0.818595	-2.356477	-0.106870
76	C	-1.357304	-3.681291	-0.223223
77	C	-0.485213	-4.776622	-0.143618
78	C	1.378076	-3.324615	0.041584
79	C	0.916393	-4.613925	0.008131
80	C	-2.836236	-5.471457	-0.495895
81	H	2.442098	-3.122362	0.119839
82	H	1.598927	-5.452644	0.065295
83	H	-3.739504	-6.045809	-0.649797
84	C	-1.509806	-1.105456	-0.084997
85	N	0.581279	-2.235552	-0.018465
86	C	-2.708005	-4.116667	-0.439127
87	H	-3.555921	-3.460447	-0.575818
88	S	-1.322643	-6.282155	-0.303281

Table S13. Cartesian coordinates of the optimized T_1 geometry of **6** computed by DFT/CPCM.

1	C	-0.849868	0.237465	-0.063480
2	C	-3.028475	-0.731628	-0.078445
3	C	-3.581866	0.550732	-0.037713
4	C	-2.750742	1.688052	0.024899
5	C	-1.365398	1.530294	0.003250
6	H	-3.702577	-1.577254	-0.145381
7	H	-3.197145	2.677856	0.053475
8	C	-0.320108	2.558775	0.069138
9	C	-0.518281	3.931412	0.160326
10	C	1.007577	2.055473	0.058989
11	C	0.568622	4.803913	0.247683
12	H	-1.527511	4.336080	0.165732
13	C	2.073330	2.936761	0.154251
14	C	1.880139	4.330040	0.250437
15	H	0.372151	5.868391	0.317737
16	H	3.088186	2.551103	0.155135
17	C	-5.053692	0.716627	-0.063057
18	C	-5.686184	1.697847	0.713208
19	C	-5.867622	-0.094649	-0.859588
20	C	-7.065503	1.851670	0.691016
21	H	-5.088847	2.333182	1.361845
22	C	-7.251309	0.062603	-0.876659
23	H	-5.411656	-0.847053	-1.497773
24	C	-7.886368	1.038537	-0.103442
25	H	-7.510980	2.620620	1.317122
26	H	-7.834758	-0.588828	-1.518874
27	Au	1.098209	0.019036	-0.109052
28	C	-9.402618	1.243378	-0.097776
29	C	-10.123695	0.261368	-1.024955
30	H	-9.953503	-0.778665	-0.727135
31	H	-11.202359	0.444912	-0.985478
32	H	-9.806081	0.377236	-2.066582
33	C	-9.939488	1.041198	1.328863
34	H	-9.489913	1.745196	2.035684
35	H	-11.024631	1.193008	1.350481
36	H	-9.729971	0.027221	1.685078
37	C	-9.725481	2.672528	-0.564305
38	H	-9.269228	3.424582	0.086554
39	H	-9.360216	2.842980	-1.582370
40	H	-10.808843	2.838006	-0.558311
41	C	3.098989	5.250799	0.348561
42	C	3.966112	5.083968	-0.910832
43	H	4.849057	5.730696	-0.851806
44	H	4.313773	4.053342	-1.033033
45	H	3.403485	5.357316	-1.809687
46	C	2.703132	6.725254	0.465128
47	H	2.136930	7.064684	-0.408575
48	H	2.101064	6.914539	1.360056
49	H	3.604861	7.342334	0.535298
50	C	3.926645	4.876819	1.589554
51	H	3.333297	4.989881	2.502825
52	H	4.282646	3.842911	1.545758
53	H	4.804042	5.528603	1.669932
54	C	4.141287	0.329874	-0.921110
55	C	3.932806	-0.515068	1.117041
56	C	3.874306	0.838785	-2.195365
57	C	5.469112	0.189868	-0.432543
58	C	3.416811	-1.029403	2.310932
59	C	5.332305	-0.366517	0.909072
60	C	4.962224	1.211443	-2.982652
61	H	2.852536	0.941906	-2.547857
62	C	6.535779	0.564054	-1.225938
63	C	4.324318	-1.395863	3.302094
64	H	2.345541	-1.138482	2.450225
65	C	6.217721	-0.734628	1.902008
66	C	6.269143	1.077270	-2.507105
67	H	4.791767	1.611316	-3.976806
68	H	7.559842	0.468399	-0.877990
69	C	5.699532	-1.251522	3.102632
70	H	3.958230	-1.799946	4.240132
71	H	7.290505	-0.632419	1.769310
72	H	7.098932	1.375474	-3.140481
73	H	6.385369	-1.545395	3.891213
74	N	3.226317	-0.097080	0.015022
75	C	-0.885160	-2.161892	-0.072377
76	C	-1.387012	-3.463027	0.217305
77	C	-0.542850	-4.565872	0.071968
78	C	1.267601	-3.105693	-0.619446
79	C	0.797940	-4.437950	-0.412914
80	C	2.557197	-2.951333	-1.161403
81	C	-2.777617	-5.200076	0.918238
82	C	1.638866	-5.525311	-0.685706
83	H	2.900702	-1.953604	-1.402922
84	C	3.373137	-4.042916	-1.423782
85	H	-3.627809	-5.748228	1.301840
86	C	2.924192	-5.340739	-1.176225
87	H	1.265771	-6.531782	-0.511009
88	H	4.362549	-3.877277	-1.841354
89	H	3.560234	-6.196094	-1.381388
90	C	-1.628685	-0.932040	-0.064863
91	N	0.481100	-2.010057	-0.334620
92	C	-2.675498	-3.859740	0.721940
93	H	-3.477026	-3.179083	0.973385
94	S	-1.326293	-6.047954	0.515446

Table S14. Cartesian coordinates of the optimized S_1 geometry of **1** computed by TDDFT/CPCM.

1	C	-0.649387	0.018154	-0.006554
2	C	-2.864689	-0.859284	0.011187
3	C	-3.361619	0.448566	-0.015090
4	C	-2.483673	1.550522	-0.036975
5	C	-1.106028	1.333391	-0.028222
6	H	-3.578812	-1.673604	0.069133
7	H	-2.888079	2.557249	-0.088953
8	C	-0.011458	2.315811	-0.046791
9	C	-0.139610	3.698541	-0.076570
10	C	1.290790	1.747427	-0.030267
11	C	0.992433	4.518020	-0.090321
12	H	-1.126688	4.154672	-0.089403
13	C	2.401810	2.576410	-0.044168
14	C	2.279282	3.980880	-0.074492
15	H	0.850392	5.593158	-0.113827
16	H	3.394188	2.133502	-0.031023
17	C	-4.825450	0.674558	-0.015731
18	C	-5.396888	1.737605	0.697510
19	C	-5.692539	-0.160231	-0.727436
20	C	-6.768943	1.947685	0.695869
21	H	-4.757154	2.393672	1.281860
22	C	-7.068574	0.053804	-0.724284
23	H	-5.284027	-0.979378	-1.313401
24	C	-7.642742	1.111986	-0.014238
25	H	-7.166244	2.779643	1.271891
26	H	-7.694775	-0.620053	-1.299553
27	Au	1.278521	-0.287583	0.010893
28	C	-9.149101	1.378692	0.013700
29	C	-9.932905	0.366283	-0.825741
30	H	-9.797840	-0.656940	-0.459628
31	H	-11.001867	0.597709	-0.774954
32	H	-9.637139	0.396270	-1.879758
33	C	-9.653889	1.295371	1.463828
34	H	-9.157600	2.026811	2.108835
35	H	-10.731390	1.492002	1.502296
36	H	-9.473552	0.300267	1.883513
37	C	-9.429614	2.784702	-0.541761
38	H	-8.927279	3.560386	0.044149
39	H	-9.086421	2.870954	-1.577974
40	H	-10.505295	2.993430	-0.520029
41	C	3.542448	4.845504	-0.087782
42	C	4.381029	4.506662	-1.331522
43	H	5.292905	5.114380	-1.351628
44	H	4.680690	3.454203	-1.345439
45	H	3.817170	4.707813	-2.248370
46	C	3.220934	6.342096	-0.121476
47	H	2.654174	6.615888	-1.017569
48	H	2.646865	6.654238	0.757254
49	H	4.152732	6.917063	-0.130045
50	C	4.369982	4.560724	1.176738
51	H	3.798254	4.801493	2.079060
52	H	4.668806	3.509765	1.238751
53	H	5.282006	5.168560	1.178529
54	C	4.193171	-0.761769	-1.079755
55	C	4.198087	-0.705292	1.125730
56	C	3.800664	-0.734334	-2.424085
57	C	5.552794	-0.958398	-0.702841
58	C	3.812526	-0.608913	2.468839
59	C	5.556087	-0.920935	0.752950
60	C	4.787177	-0.908929	-3.390088
61	H	2.760912	-0.580026	-2.692877
62	C	6.517677	-1.129836	-1.674490
63	C	4.804182	-0.732882	3.437530
64	H	2.774461	-0.441487	2.736146
65	C	6.526074	-1.041282	1.727188
66	C	6.121435	-1.103632	-3.024038
67	H	4.517153	-0.893247	-4.440446
68	H	7.560733	-1.282091	-1.415095
69	C	6.136738	-0.945486	3.075537
70	H	4.539247	-0.663113	4.486993
71	H	7.567935	-1.205849	1.470544
72	H	6.871176	-1.237202	-3.797111
73	H	6.890418	-1.038441	3.850726
74	N	3.393413	-0.613397	0.021585
75	C	-0.788186	-2.384814	0.032346
76	C	-1.330136	-3.679005	0.030230
77	C	-0.519694	-4.837215	0.056936
78	C	1.391561	-3.384125	0.078857
79	C	0.899099	-4.657069	0.085492
80	C	-1.276834	-6.037066	0.046326
81	C	-2.625929	-5.825762	0.010826
82	H	2.461385	-3.205085	0.095802
83	H	1.573333	-5.505252	0.108943
84	H	-0.829705	-7.024991	0.064530
85	H	-3.424294	-6.553955	-0.002339
86	C	-1.477440	-1.118646	0.009038
87	S	-3.015390	-4.132472	-0.011764
88	N	0.616928	-2.270141	0.052200

Table S15. Cartesian coordinates of the optimized T_1 geometry of **1** computed by TDDFT/CPCM.

1	C	-0.649009	0.017633	-0.007654
2	C	-2.864672	-0.859257	0.010583
3	C	-3.361375	0.448674	-0.014858
4	C	-2.483145	1.550410	-0.036433
5	C	-1.105602	1.332977	-0.028067
6	H	-3.578908	-1.673461	0.068800
7	H	-2.887331	2.557263	-0.087742
8	C	-0.010962	2.315260	-0.045661
9	C	-0.138939	3.698034	-0.074558
10	C	1.291195	1.746786	-0.029013
11	C	0.993168	4.517410	-0.087399
12	H	-1.125975	4.154248	-0.087416
13	C	2.402364	2.575640	-0.041882
14	C	2.279954	3.980125	-0.071431
15	H	0.851240	5.592574	-0.110303
16	H	3.394707	2.132716	-0.028556
17	C	-4.825145	0.675018	-0.014822
18	C	-5.396054	1.737917	0.699065
19	C	-5.692702	-0.159255	-0.726562
20	C	-6.768052	1.948366	0.697979
21	H	-4.755953	2.393572	1.283476
22	C	-7.068678	0.055149	-0.722850
23	H	-5.284608	-0.978273	-1.313000
24	C	-7.642316	1.113198	-0.012180
25	H	-7.164931	2.780201	1.274470
26	H	-7.695259	-0.618305	-1.298179
27	Au	1.279044	-0.288332	0.010375
28	C	-9.148584	1.380349	0.016308
29	C	-9.932924	0.368587	-0.823412
30	H	-9.798023	-0.654861	-0.457866
31	H	-11.001806	0.600280	-0.772177
32	H	-9.637477	0.399036	-1.877504
33	C	-9.653014	1.296490	1.466530
34	H	-9.156347	2.027479	2.111756
35	H	-10.730447	1.493420	1.505369
36	H	-9.472863	0.301133	1.885697
37	C	-9.428800	2.786716	-0.538402
38	H	-8.926041	3.561955	0.047737
39	H	-9.085876	2.873354	-1.574672
40	H	-10.504406	2.995784	-0.516260
41	C	3.543237	4.844600	-0.083840
42	C	4.382115	4.506350	-1.327546
43	H	5.294110	5.113910	-1.347014
44	H	4.681579	3.453841	-1.342024
45	H	3.818558	4.708175	-2.244433
46	C	3.221906	6.341249	-0.116776
47	H	2.655451	6.615625	-1.012882
48	H	2.647619	6.652959	0.761964
49	H	4.153778	6.916102	-0.124739
50	C	4.370387	4.559003	1.180744
51	H	3.798419	4.799245	2.083053
52	H	4.669166	3.508000	1.242202
53	H	5.282434	5.166800	1.183158
54	C	4.194400	-0.754447	-1.079061
55	C	4.194914	-0.713557	1.127022
56	C	3.804792	-0.717757	-2.423910
57	C	5.553370	-0.952108	-0.700733
58	C	3.806685	-0.626921	2.469969
59	C	5.553765	-0.925011	0.755311
60	C	4.793632	-0.884018	-3.389048
61	H	2.765445	-0.562862	-2.694015
62	C	6.520633	-1.115348	-1.671499
63	C	4.796593	-0.756644	3.439681
64	H	2.767874	-0.462418	2.736294
65	C	6.522037	-1.051296	1.730566
66	C	6.127345	-1.079769	-3.021612
67	H	4.525778	-0.860981	-4.439830
68	H	7.563289	-1.268212	-1.410856
69	C	6.130056	-0.965392	3.078744
70	H	4.529589	-0.694468	4.489098
71	H	7.564549	-1.213021	1.474760
72	H	6.878888	-1.206802	-3.794041
73	H	6.882351	-1.063055	3.854704
74	N	3.392065	-0.615026	0.021888
75	C	-0.788645	-2.385256	0.029477
76	C	-1.330985	-3.679249	0.024342
77	C	-0.520941	-4.837771	0.049092
78	C	1.390837	-3.385380	0.074934
79	C	0.897816	-4.658036	0.078712
80	C	-1.278421	-6.037411	0.035394
81	C	-2.627379	-5.825621	-0.000530
82	H	2.460694	-3.206804	0.092703
83	H	1.571803	-5.506473	0.100761
84	H	-0.831585	-7.025502	0.051791
85	H	-3.425956	-6.553545	-0.015673
86	C	-1.477489	-1.118855	0.007552
87	S	-3.016361	-4.132138	-0.019948
88	N	0.616440	-2.270930	0.050586

OLED Fabrication and Characterization

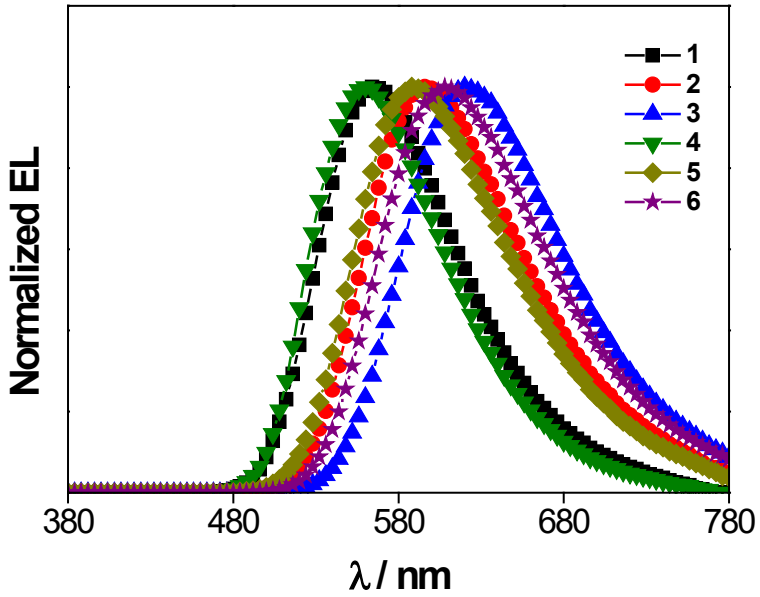

Figure S26. Normalized EL spectra of the solution-processed devices based on **1**−**6**.

Table S16. Key parameters of solution-processed devices based on **1**−**6**.

Complex	Conc. / wt%	CE[a] / cd A^{-1}	PE[b] / lm W^{-1}	EQE[c] / %	λ_{max}[d] / nm	CIE[e] (x, y)
1	5	12.6	2.6	3.7	544	0.39, 0.57
	10	25.2	7.4	7.9	560	0.44, 0.54
	15	26.1	9.3	8.6	564	0.46, 0.52
	20	22.4	8.9	8.0	572	0.49, 0.50
2	5	8.6	1.7	3.3	580	0.51, 0.48
	10	10.8	2.8	4.7	588	0.53, 0.46
	15	9.4	3.4	4.7	596	0.55, 0.44
	20	2.0	0.6	1.1	600	0.56, 0.43
3	5	2.7	0.6	1.5	608	0.57, 0.43
	10	3.9	1.0	2.4	616	0.59, 0.41
	15	6.2	2.3	4.5	620	0.61, 0.39
	20	5.8	2.5	4.6	628	0.62, 0.38
4	5	13.4	3.5	3.9	544	0.39, 0.58
	10	25.6	9.9	7.9	560	0.44, 0.55
	15	27.0	10.6	8.5	560	0.45, 0.54
	20	25.9	11.4	8.4	564	0.46, 0.53
5	5	9.1	1.8	3.2	572	0.48, 0.51
	10	12.2	3.7	4.8	580	0.51, 0.48
	15	11.8	4.4	5.2	588	0.54, 0.46
	20	9.6	4.1	4.6	596	0.55, 0.45
6	5	8.9	2.1	3.8	588	0.53, 0.46
	10	12.0	3.6	6.2	600	0.56, 0.44
	15	10.1	3.8	6.0	608	0.58, 0.42
	20	9.2	4.0	5.9	612	0.59, 0.41

[a] CE represents maximum current efficiency.

[b] PE represents maximum power efficiency.

[c] EQE represents maximum external quantum efficiency.

[d] λ_{max} represents peak maximum.

[e] CIE coordinates are taken at a current density of 100 cd m^{-2}.

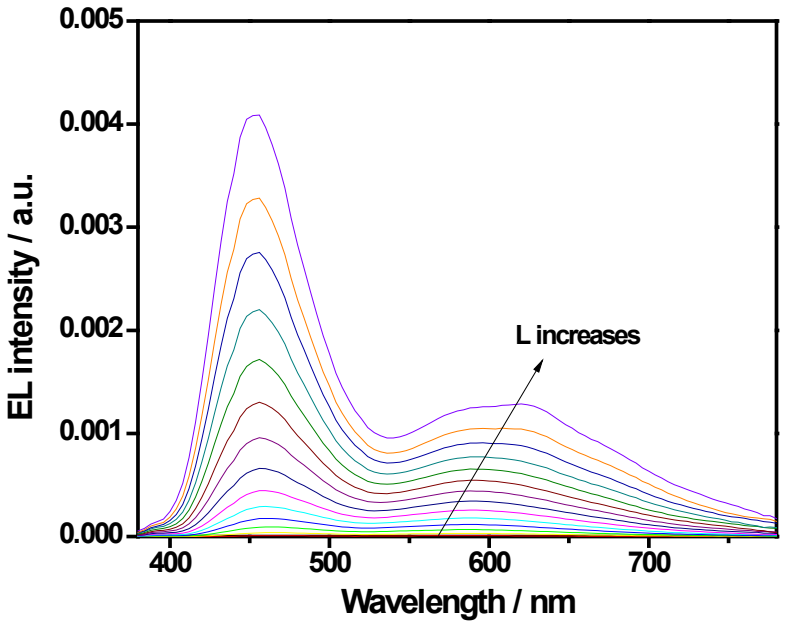

Figure S27. EL spectra of vacuum-deposited devices based on **6**.

Table S17. Key parameters of vacuum-deposited devices based on **1**–**5**.

Complex	Conc. / % v/v	CE[a] / cd A^{-1}	PE[b] / lm W^{-1}	EQE[c] / %	λ_{max}[d] / nm	CIE[e] (x, y)
1	2	35.1	31.5	12.0	560	0.44, 0.53
	5	36.3	32.6	13.5	572	0.47, 0.51
	8	36.5	35.8	14.3	576	0.49, 0.50
	11	33.9	33.0	13.8	580	0.50, 0.49
	14	31.2	31.8	13.7	588	0.52, 0.47
2	2	11.6	10.4	6.3	600	0.54, 0.45
	5	11.6	10.4	6.8	608	0.56, 0.44
	8	10.5	9.5	7.1	612	0.57, 0.43
	11	9.5	8.5	7.0	620	0.58, 0.41
	14	8.7	7.5	6.4	620	0.59, 0.41
3	2	11.2	10.1	7.6	620	0.58, 0.41
	5	9.2	8.2	8.2	628	0.60, 0.40
	8	7.5	6.7	7.3	636	0.61, 0.39
	11	6.5	5.7	6.9	636	0.62, 0.38
4	2	38.1	34.2	12.6	556	0.43, 0.54
	5	41.6	37.3	14.3	564	0.45, 0.53
	8	40.4	36.2	14.4	564	0.46, 0.53
	11	38.3	36.3	14.5	568	0.47, 0.52
	14	34.9	33.2	13.5	572	0.48, 0.51
5	2	15.2	11.9	6.5	588	0.51, 0.48
	5	17.8	16.0	8.5	588	0.52, 0.47
	8	17.2	15.4	8.3	596	0.53, 0.46
	11	16.1	14.4	8.7	600	0.54, 0.45
	14	14.5	13.0	8.2	600	0.54, 0.45

[a] CE represents maximum current efficiency.

[b] PE represents maximum power efficiency.

[c] EQE represents maximum external quantum efficiency.

[d] λ_{max} represents peak maximum.

[e] CIE coordinates are taken at a current density of 100 cd m^{-2}.

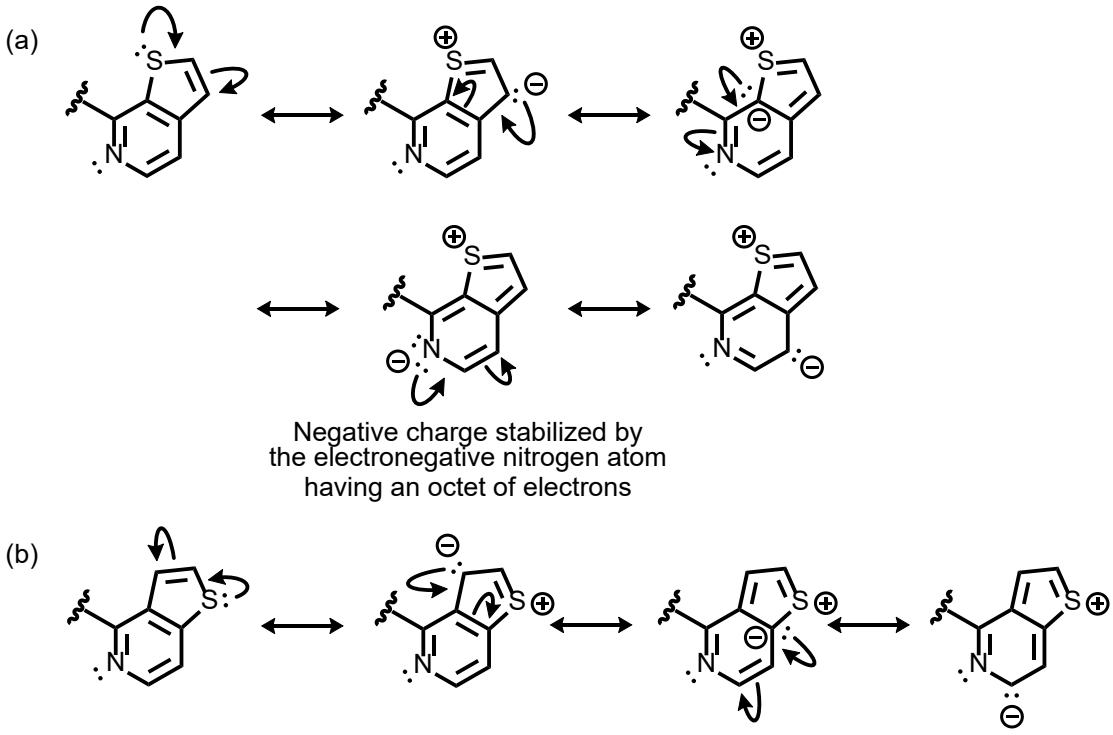

Figure S28. Resonance structures of thieno[2,3-*c*]pyridine (1-thpy) and thieno[3,2-*c*]pyridine (2-thpy) moieties in the cyclometalating ligands.

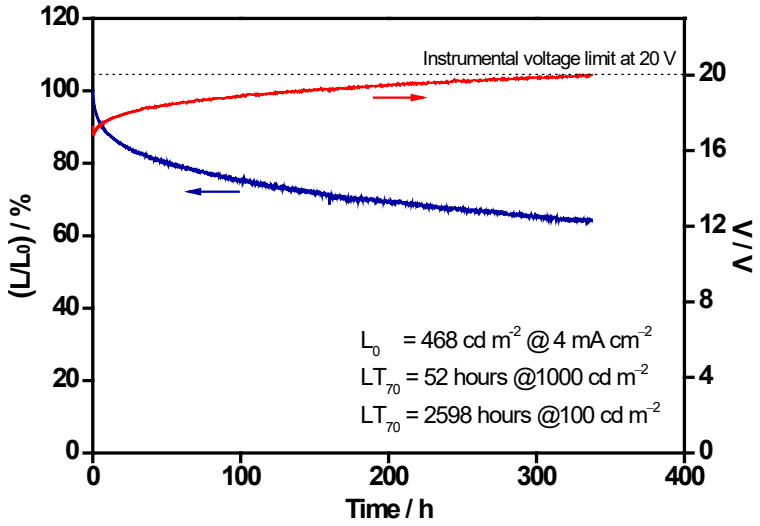

Figure S29. Relative luminance, L/L_0, and driving voltage of the solution-processed device based on **1** as a function of operation projected at an initial luminance of 100 cd cm^{-2}.

Table S18. Lifetime data of devices based on **1**–**5**.

Complex	L_0[a] / cd m^{-2}	Lifetime / h		
		LT_{70}[b] at L_0	LT_{70} at 1,000 cd m^{-2}	LT_{70} at 100 cd m^{-2}
Vacuum-deposited devices				
1	4,869	85.6	1,262	63,258
2	1,291	203.7	314	15,760
3	993	680	672	33,676
4	3,534	0.2	2	86
5	1,596	0.5	1	55
Solution-processed device				
1	468	188	52	2,598

[a] L_0 is defined as the initial luminance.

[b] LT_{70} is defined as the operational lifetime at 70 % of the initial luminance.

Materials and reagents. Potassium tetrachloroaurate(III) and sodium hydride were purchased from Strem Chemicals, Inc. Carbazole was purchased from Sigma-Aldrich. 3,6-Di-*tert*-butylcarbazole was purchased from Alfa Aesar. All solvents for synthesis were purified by the Pure Solv MD System (Multiple Dispensing System, Innovative Technology) before use. All other reagents were of analytical grade and were used as received. Tetra-*n*-butylammonium hexafluorophosphate (Aldrich, 98 %) was recrystallized for no less than three times from hot absolute ethanol prior to use. All reactions were performed under anaerobic and anhydrous conditions using standard Schlenk techniques under an inert atmosphere of nitrogen.

Physical measurements and instrumentation. The UV−vis absorption spectra were recorded on a Cary 60 UV−vis (Agilent Technology) spectrophotometer equipped with a Xenon flash lamp. ^{1}H and ^{13}C{^{1}H} NMR spectra were recorded on a Bruker AVANCE 400 (400 MHz for ^{1}H nucleus) or Bruker AVANCE 500 (500 MHz for ^{1}H and 125 MHz for ^{13}C nuclei) Fourier-transform NMR spectrometer with chemical shifts reported relative to tetramethylsilane (δ = 0 ppm) in deuterated chloroform. High-resolution ESI and CSI mass spectra were recorded on Bruker maXis II^{TM} High Resolution LC-QTOF Mass Spectrometer. Elemental analyses were performed on the Carlo Erba 1106 elemental analyzer at the Institute of Chemistry, Chinese Academy of Sciences in Beijing. Steady-state excitation and emission spectra were recorded on a Horiba Scientific FluoroMax-4 fluorescence spectrofluorometer equipped with a R928P PMT detector. Liquid nitrogen was placed into the quartz-walled optical Dewar flask for low temperature (77 K) photophysical measurements. Solid-state photophysical measurements were performed with solid sample loaded into a quartz tube inside a quartz-walled Dewar flask. Low temperature (77 K) photophysical measurements were done by placing liquid nitrogen into the optical Dewar flask. Excited-state lifetimes of solution and glass samples were measured with a conventional nanosecond pulsed laser system. The excitation source used was the 355 nm output (third harmonic, 8 ns) of a Spectra-Physics Quanta-Ray Q-switched GCR-150 pulsed Nd:YAG laser (10 Hz). Luminescence decay signals were recorded by a Hamamatsu R928 photomultiplier tube, recorded on a Tektronix model TDS-620A (500 MHz, 2 GSs^{-1}) digital oscilloscope, and analyzed with a program for exponential fits. Time-resolved emission spectra were obtained using an Edinburgh Instrument LP980KS transient absorption spectrometer equipped with R928P photomultiplier tube, with capability for time-resolved emission

measurements. Relative photoluminescence quantum yields in solution were measured by the optical dilute method reported by Demas and Crosby.[12] A solution of quinine sulfate in 0.5 M H_2SO_4 has been used as reference (Φ = 0.546, excitation wavelength at 365 nm),[12] whereas absolute PLQYs in thin films were measured on a Hamamatsu C9920−03 absolute PLQY measurement system. Excited-state lifetimes of thin films were measured on a Quantaurus-Tau C11367−34 fluorescence lifetime spectrometer. Cyclic voltammetry was performed with a CH Instruments Model CHI620E (CH Instruments, Inc.). All solutions for electrochemical measurements were purged with prepurified argon gas prior to measurement. Thermal analyses were performed on a TGA Q50 (TA Instruments), in which T_d is defined as the temperature at which the sample shows a 5 % weight loss.

Synthesis. The cyclometalating ligands incorporated with thienopyridine moieties, 4-^{t}BuC^C(4-^{t}BuC$_6$H$_4$)^N$_{(1\text{-thpy})}$ and 4-^{t}BuC^C(4-^{t}BuC$_6$H$_4$)^N$_{(2\text{-thpy})}$,[13,14] and those with the thienoquinoline moieties, 4-^{t}BuC^C(4-^{t}BuC$_6$H$_4$)^N$_{(1\text{-thq})}$ and 4-^{t}BuC^C(4-^{t}BuC$_6$H$_4$)^N$_{(2\text{-thq})}$,[15] were synthesized by slight modifications of the literature procedures. The resulting ligands were then mercurated and transmetalated to gold(III) metal center to afford the cyclometalated chlorogold(III) precursor complexes, [Au{4-^{t}BuC^C(4-^{t}BuC$_6$H$_4$)^N$_{(1\text{-thpy})}$}Cl], [Au{4-^{t}BuC^C(4-^{t}BuC$_6$H$_4$)^N$_{(2\text{-thpy})}$}Cl], [Au{4-^{t}BuC^C(4-^{t}BuC$_6$H$_4$)^N$_{(1\text{-thq})}$}Cl] and [Au{4-^{t}BuC^C(4-^{t}BuC$_6$H$_4$)^N$_{(2\text{-thq})}$}Cl], which were prepared according to modification of the previously reported literature procedures.[13,14] The carbazolylgold(III) complexes were then synthesized by reacting carbazole or 3,6-di-*tert*-butylcarbazole with the corresponding chlorogold(III) precursors with sodium hydride in degassed tetrahydrofuran.[14,16]

4-^{t}BuC^C(4-^{t}BuC$_6$H$_4$)^N$_{(1\text{-thq})}$

Off-white solid. Yield: 609 mg, 45 %. ^{1}H NMR (400 MHz, $CDCl_3$, 298 K, relative to Me_4Si, δ/ppm): δ 8.35−8.31 (m, 4H, thienoquinolinyl protons and phenyl protons), 8.10−8.09 (d, J = 5.4 Hz, 1H, thienoquinolinyl proton), 7.98−7.97 (m, 1H, phenyl proton), 7.91−7.90 (d, J = 5.4 Hz, 1H, thienoquinolinyl proton), 7.78−7.76 (m, 1H, thienoquinolinyl proton), 7.74−7.70 (d, J = 8.4 Hz, 4H, phenyl protons), 7.70−7.65 (m, 1H, thienoquinolinyl proton), 7.54−7.51 (d, J = 8.4 Hz, 4H, phenyl protons), 1.39 (s, 18H, −^{t}Bu). HRMS (Positive ESI): Found m/z 524.2592 $[M]^+$. Calcd for $C_{38}H_{36}S$ $[M]^+$:

m/z 524.2538.

4-^{t}BuC^C(4-^{t}BuC$_6$H$_4$)^N$_{(2\text{-thq})}$

Pale yellow solid. Yield: 707 mg, 49 %. ^{1}H NMR (400 MHz, $CDCl_3$, 298 K, relative to Me_4Si, δ/ppm): δ 8.30−8.28 (d, J = 8.4 Hz, 1H, thienoquinolinyl proton), 8.18−8.16 (d, J = 8.1 Hz, 1H, thienoquinolinyl proton), 8.08 (d, J = 1.7 Hz, 2H, phenyl protons), 7.95 (m, 1H, phenyl proton), 7.77−7.72 (m, 2H, thienoquinolinyl protons), 7.69−7.67 (d, J = 8.4 Hz, 4H, phenyl protons), 7.66−7.62 (m, 1H, thienoquinolinyl proton), 7.57−7.56 (d, J = 5.4 Hz, 1H, thienoquinolinyl proton), 7.52−7.50 (d, J = 8.4 Hz, 4H, phenyl protons), 1.38 (s, 18H, −^{t}Bu). HRMS (Positive ESI): Found *m/z* 524.2585 $[M]^+$. Calcd for $C_{38}H_{36}S$ $[M]^+$: *m/z* 524.2538.

[Au{4-^{t}BuC^C(4-^{t}BuC$_6$H$_4$)^N$_{(1\text{-thpy})}$}Cl]

Yellow solid. Yield: 308 mg, 78 %. ^{1}H NMR (400 MHz, $CDCl_3$, 298 K, relative to Me_4Si, δ/ppm): δ 9.15−9.14 (d, J = 6.0 Hz, 1H, thienopyridyl proton), 8.03−8.02 (d, J = 5.4 Hz, 1H, thienopyridyl proton), 8.00 (d, J = 1.9 Hz, 1H, phenyl proton), 7.97 (d, J = 1.5 Hz, 1H, phenyl proton), 7.88−7.86 (d, J = 6.0 Hz, 1H, thienopyridyl proton), 7.66−7.64 (d, J = 8.5 Hz, 2H, phenyl protons), 7.56−7.55 (d, J = 8.5 Hz, 2H, phenyl protons), 7.53−7.52 (m, 2H, thienopyridyl proton and phenyl proton), 7.32−7.30 (d, J = 8.0 Hz, 1H, phenyl proton), 7.25−7.24 (m, 1H, phenyl proton), 1.41 (s, 9H, −^{t}Bu), 1.38 (s, 9H, −^{t}Bu). HRMS (Positive ESI): Found *m/z* 711.2125 $[M-Cl+CH_3CN]^+$. Calcd for $AuC_{35}H_{34}N_2S$ $[M-Cl+CH_3CN]^+$: *m/z* 711.2102.

[Au{4-^{t}BuC^C(4-^{t}BuC$_6$H$_4$)^N$_{(2\text{-thpy})}$}Cl]

Yellow solid. Yield: 219 mg, 71 %. ^{1}H NMR (500 MHz, $CDCl_3$, 298 K, relative to Me_4Si, δ/ppm): δ 9.09−9.08 (d, J = 6.1 Hz, 1H, thienopyridyl proton), 8.25−8.24 (d, J = 5.7 Hz, 1H, thienopyridyl proton), 7.98−7.97 (m, 2H, phenyl protons), 7.94−7.93 (d, J = 6.1 Hz, 1H, thienopyridyl proton), 7.83−7.82 (d, J = 5.7 Hz, 1H, thienopyridyl proton), 7.64−7.62 (d, J = 8.4 Hz, 2H, phenyl protons), 7.56−7.55 (d, J = 8.4 Hz, 2H, phenyl protons), 7.47−7.46 (d, J = 1.4 Hz, 1H, phenyl proton), 7.30−7.28 (d, J = 8.0 Hz, 1H, phenyl proton), 7.25−7.23 (m, 1H, phenyl proton), 1.41 (s, 9H, −^{t}Bu), 1.36 (s, 9H, −^{t}Bu). HRMS (Positive ESI): Found *m/z* 711.2089 $[M-Cl+CH_3CN]^+$. Calcd for $AuC_{35}H_{34}N_2S$ $[M-Cl+CH_3CN]^+$: *m/z* 711.2102.

[Au{4-^{t}BuC^C(4-^{t}BuC$_6$H$_4$)^N$_{(1\text{-thq})}$}Cl]

Yellow solid. Yield: 303 mg, 65 %. ^{1}H NMR (500 MHz, $CDCl_3$, 298 K, relative to Me_4Si, δ/ppm): δ 10.0−9.99 (d, J = 8.8 Hz, 1H, thienoquinolinyl proton), 8.24 (d, J = 1.6 Hz, 1H, phenyl proton), 8.18 (s, 1H, phenyl proton), 8.15−8.14 (d, J = 7.9 Hz, 1H, thienoquinolinyl proton), 8.05−8.04 (d, J = 5.4 Hz, 1H, thienoquinolinyl proton), 7.93−7.92 (d, J = 5.4 Hz, 1H, thienoquinolinyl proton), 7.74−7.71 (m, 1H, thienoquinolinyl proton), 7.62−7.59 (m, 3H, thienoquinolinyl proton and phenyl protons), 7.54−7.52 (d, J = 8.3 Hz, 2H, phenyl protons), 7.41 (s, 1H, phenyl proton), 7.24−7.23 (d, J = 1.6 Hz, 1H, phenyl proton), 7.22−7.21 (d, J = 7.9 Hz, 1H, phenyl proton), 1.42 (s, 9H, −^{t}Bu), 1.41 (s, 9H, −^{t}Bu). HRMS (Positive ESI): Found m/z 761.2286 $[M-Cl+CH_3CN]^+$. Calcd for $AuC_{39}H_{36}N_2S$ $[M-Cl+CH_3CN]^+$: m/z 761.2259.

[Au{4-^{t}BuC^C(4-^{t}BuC$_6$H$_4$)^N$_{(2\text{-thq})}$}Cl]

Yellow solid. Yield: 173 mg, 61 %. ^{1}H NMR (500 MHz, $CDCl_3$, 298 K, relative to Me_4Si, δ/ppm): δ 9.90−9.88 (d, J = 8.8 Hz, 1H, thienoquinolinyl proton), 8.31−8.30 (d, J = 5.6 Hz, 1H, thienoquinolinyl proton), 8.15 (s, 1H, phenyl proton), 8.01−7.99 (m, 2H, thienoquinolinyl proton and phenyl proton), 7.73−7.71 (m, 1H, thienoquinolinyl proton), 7.65−7.57 (m, 4H, thienoquinolinyl protons and phenyl protons), 7.55−7.53 (d, J = 8.3 Hz, 2H, phenyl protons), 7.32 (s, 1H, phenyl proton), 7.23−7.18 (m, 2H, phenyl protons), 1.41 (s, 9H, −^{t}Bu), 1.35 (s, 9H, −^{t}Bu). HRMS (Positive ESI): Found m/z 761.2237 $[M-Cl+CH_3CN]^+$. Calcd for $AuC_{39}H_{36}N_2S$ $[M-Cl+CH_3CN]^+$: m/z 761.2259.

[Au{4-^{t}BuC^C(4-^{t}BuC$_6$H$_4$)^N$_{(1\text{-thpy})}$}(Cbz)] (1)

Yellow solid. Yield: 173 mg, 73 %. ^{1}H NMR (500 MHz, $CDCl_3$, 298 K, relative to Me_4Si, δ/ppm): δ 8.28−8.26 (d, J = 7.7 Hz, 2H, carbazolyl protons), 8.14−8.12 (m, 2H, phenyl proton and carbazolyl proton), 8.06−8.05 (d, J = 5.4 Hz, 1H, thienopyridyl proton), 7.72−7.70 (m, 2H, thienopyridyl proton and phenyl proton), 7.67−7.65 (m, 3H, phenyl protons and carbazolyl proton), 7.60−7.58 (m, 3H, thienopyridyl proton and phenyl protons), 7.51−7.50 (d, J = 5.4 Hz, 1H, thienopyridyl proton), 7.39−7.38 (d, J = 8.0 Hz, 1H, phenyl proton), 7.31−7.28 (m, 2H, carbazolyl protons), 7.19−7.17 (dd, J = 8.0 and 1.9 Hz, 1H, phenyl proton), 7.14−7.13 (m, 2H, carbazolyl protons), 6.77−6.76 (d, J = 1.9 Hz, 1H, phenyl proton), 1.43 (s, 9H, −^{t}Bu), 0.91 (s, 9H, −^{t}Bu). ^{13}C{^{1}H} NMR (125 MHz, $CDCl_3$, 298 K, relative to Me_4Si, δ/ppm): δ 166.06, 159.96, 151.83, 151.63,

151.50, 151.01, 149.17, 148.33, 148.14, 142.70, 142.00, 141.88, 138.42, 136.45, 132.43, 132.09, 126.97, 126.05, 125.34, 124.78, 124.00, 123.50, 122.96, 121.97, 121.66, 119.96, 118.37, 116.24, 113.76, 67.99, 65.86, 34.72, 34.68, 25.62. HRMS (Positive ESI): Found *m/z* 836.2475 $[M]^+$. Calcd for $AuC_{45}H_{39}N_2S$ $[M]^+$: *m/z* 836.2494. Elemental analyses: Found (%): C 63.27, H 4.71, N 3.35. Calcd for $C_{45}H_{39}AuN_2S \cdot H_2O$: C 63.23, H 4.83, N 3.25.

[Au{4-^{t}BuC^C(4-^{t}BuC$_6$H$_4$)^N$_{(1\text{-thpy})}$}(^{t}Bu$_2$Cbz)] (**2**)

Orange solid. Yield: 101 mg, 78 %. ^{1}H NMR (500 MHz, $CDCl_3$, 298 K, relative to Me_4Si, δ/ppm): δ 8.36−8.35 (d, J = 5.9 Hz, 1H, thienopyridyl proton), 8.24 (d, J = 1.3 Hz, 2H, carbazolyl protons), 8.13 (s, 1H, phenyl proton), 8.05−8.04 (d, J = 5.3 Hz, 1H, thienopyridyl proton), 7.71−7.70 (d, J = 8.2 Hz, 2H, phenyl protons), 7.66−7.64 (m, 2H, thienopyridyl proton and phenyl proton), 7.59−7.57 (d, J = 8.2 Hz, 2H, phenyl protons), 7.53−7.51 (m, 3H, thienopyridyl proton and carbazolyl protons), 7.36−7.32 (m, 3H, phenyl proton and carbazolyl protons), 7.15−7.13 (dd, J = 6.4 and 1.5 Hz, 1H, phenyl proton), 6.65 (d, J = 1.5 Hz, 1H, phenyl proton), 1.47 (s, 18H, −^{t}Bu), 1.43 (s, 9H, −^{t}Bu), 0.88 (s, 9H, −^{t}Bu). ^{13}C{^{1}H} NMR (125 MHz, $CDCl_3$, 298 K, relative to Me_4Si, δ/ppm): δ 166.44, 160.04, 151.81, 151.56, 151.41, 150.94, 149.17, 148.05, 147.01, 142.97, 142.06, 141.77, 138.86, 138.55, 136.33, 132.40, 132.30, 126.98, 126.03, 125.21, 124.59, 123.51, 122.93, 121.93, 121.81, 121.48, 118.37, 115.57, 113.21, 67.98, 65.86, 34.70, 34.68, 34.60, 32.26, 32.03, 31.41, 30.74, 29.73. HRMS (Positive ESI): Found *m/z* 948.3709 $[M]^+$. Calcd for $AuC_{53}H_{55}N_2S$ $[M]^+$: *m/z* 948.3746. Elemental analyses: Found (%): C 65.14, H 5.74, N 2.93. Calcd for $C_{53}H_{55}AuN_2S \cdot 1.5H_2O$: C 65.22, H 5.99, N 2.87.

[Au{4-^{t}BuC^C(4-^{t}BuC$_6$H$_4$)^N$_{(1\text{-thq})}$}(Cbz)] (**3**)

Orange solid. Yield: 201 mg, 74 %. ^{1}H NMR (400 MHz, CD_2Cl_2, 298 K, δ/ppm): δ 8.79−8.77 (d, J = 8.6 Hz, 1H, thienoquinolinyl proton), 8.45 (d, J = 1.4 Hz, 1H, phenyl proton), 8.28−8.25 (m, 3H, thienoquinolinyl proton and carbazolyl protons), 8.20−8.19 (d, J = 5.4 Hz, 1H, thienoquinolinyl proton), 8.12−8.10 (d, J = 5.5 Hz, 1H, thienoquinolinyl proton), 7.75−7.72 (d, J = 8.4 Hz, 2H, phenyl protons), 7.68 (d, J = 1.3 Hz, 1H, phenyl proton), 7.63−7.61 (d, J = 8.1 Hz, 2H, carbazolyl protons), 7.59−7.56 (d, J = 8.4 Hz, 2H, phenyl protons), 7.45−7.41 (t, J = 8.0 Hz, 1H,

thienoquinolinyl proton), 7.32−7.30 (d, *J* = 8.0 Hz, 1H, phenyl proton), 7.27−7.23 (m, 2H, carbazolyl protons), 7.13−7.05 (m, 3H, phenyl proton and carbazolyl protons), 6.98−6.93 (m, 1H, thienoquinolinyl proton), 5.62 (d, *J* = 1.9 Hz, 1H, phenyl proton), 1.40 (s, 9H, −^{t}Bu), 0.70 (s, 9H, −^{t}Bu). $^{13}C\{^1H\}$ NMR (125 MHz, CD_2Cl_2, 298 K, *δ*/ppm): *δ* 167.51, 161.88, 152.12, 151.72, 151.57, 151.56, 149.25, 148.92, 147.24, 144.40, 144.09, 142.19, 138.48, 137.08, 130.97, 130.77, 129.86, 128.41, 128.18, 127.34, 126.62, 126.52, 125.31, 124.75, 124.65, 124.56, 123.86, 122.43, 122.29, 122.10, 120.32, 117.15, 114.41, 35.10, 35.03, 31.67, 30.79. HRMS (Positive ESI): Found *m*/*z* 886.2673 $[M]^+$. Calcd for $AuC_{49}H_{41}N_2S$ $[M]^+$: *m*/*z* 886.2650. Elemental analyses: Found (%): C 63.64, H 4.62, N 3.09. Calcd for $C_{49}H_{41}AuN_2S\cdot 2H_2O$: C 63.77, H 4.91, N 3.04.

[Au{4-^{t}BuC^C(4-^{t}BuC$_6$H$_4$)^N$_{(2\text{-thpy})}$}(Cbz)] (4)

Yellow solid. Yield: 113 mg, 68 %. ^1H NMR (500 MHz, $CDCl_3$, 298 K, relative to Me_4Si, *δ*/ppm): *δ* 8.34−8.33 (d, *J* = 5.8 Hz, 1H, thienopyridyl proton), 8.27−8.26 (m, 2H, carbazolyl protons), 8.10−8.08 (m, 2H, phenyl proton and carbazolyl proton), 7.85−7.84 (d, *J* = 5.7 Hz, 1H, thienopyridyl proton), 7.70−7.63 (m, 6H, thienopyridyl proton and phenyl protons and carbazolyl proton), 7.59−7.57 (m, 2H, thienopyridyl proton and phenyl proton), 7.38−7.36 (d, *J* = 8.0 Hz, 1H, phenyl proton), 7.31−7.27 (m, 2H, carbazolyl protons), 7.18−7.16 (dd, *J* = 8.0 and 1.9 Hz, 1H, phenyl proton), 7.14−7.11 (m, 2H, carbazolyl protons), 6.73 (d, *J* = 1.9 Hz, 1H, phenyl proton), 1.43 (s, 9H, −^{t}Bu), 0.90 (s, 9H, −^{t}Bu). $^{13}C\{^1H\}$ NMR (125 MHz, $CDCl_3$, 298 K, relative to Me_4Si, *δ*/ppm): *δ* 166.11, 160.32, 152.83, 151.77, 151.73, 151.61, 151.00, 148.31, 148.23, 142.87, 142.09, 141.31, 138.71, 132.89, 132.05, 131.15, 127.05, 126.02, 125.34, 124.76, 124.00, 123.42, 122.16, 122.08, 121.60, 119.95, 118.07, 116.25, 113.72, 67.98, 65.86, 34.68, 25.62. HRMS (Positive ESI): Found *m*/*z* 836.2471 $[M]^+$. Calcd for $AuC_{45}H_{39}N_2S$ $[M]^+$: *m*/*z* 836.2494. Elemental analyses: Found (%): C 64.17, H 4.78, N 3.42. Calcd for $C_{45}H_{39}AuN_2S$: C 64.59, H 4.70, N 3.35.

[Au{4-^{t}BuC^C(4-^{t}BuC$_6$H$_4$)^N$_{(2\text{-thpy})}$}(^{t}Bu$_2$Cbz)] (5)

Orange solid. Yield: 88 mg, 82 %. ^1H NMR (500 MHz, $CDCl_3$, 298 K, relative to Me_4Si, *δ*/ppm): *δ* 8.34−8.33 (d, *J* = 5.8 Hz, 1H, thienopyridyl proton), 8.31−8.30 (d, *J* = 6.1 Hz, 1H, thienopyridyl proton), 8.24 (d, *J* = 1.9 Hz, 2H, carbazolyl protons), 8.10 (d, *J*

= 1.0 Hz, 1H, phenyl proton), 7.85−7.84 (d, *J* = 5.8 Hz, 1H, thienopyridyl proton), 7.75−7.74 (d, *J* = 6.1 Hz, 1H, thienopyridyl proton), 7.67−7.65 (d, *J* = 8.3 Hz, 2H, phenyl protons), 7.61 (d, *J* = 0.9 Hz, 1H, phenyl proton), 7.59−7.57 (d, *J* = 8.3 Hz, 2H, phenyl protons), 7.52−7.50 (d, *J* = 8.5 Hz, 2H, carbazolyl protons), 7.35−7.32 (m, 3H, phenyl proton and carbazolyl protons), 7.14−7.12 (dd, *J* = 8.0 and 1.9 Hz, 1H, phenyl proton), 6.62−6.61 (d, *J* = 1.9 Hz, 1H, phenyl proton), 1.47 (s, 18H, −^{t}Bu), 1.42 (s, 9H, −^{t}Bu), 0.87 (s, 9H, −^{t}Bu). $^{13}C\{^1H\}$ NMR (125 MHz, $CDCl_3$, 298 K, relative to Me_4Si, *δ*/ppm): *δ* 166.51, 160.40, 152.81, 151.80, 151.42, 150.95, 148.17, 147.02, 142.93, 141.99, 141.59, 138.91, 138.83, 132.88, 132.29, 131.04, 127.07, 126.02, 125.25, 124.59, 123.39, 122.12, 121.84, 121.45, 118.04, 115.60, 113.20, 34.70, 34.62, 32.27, 31.43, 30.76. HRMS (Positive ESI): Found *m/z* 948.3710 $[M]^+$. Calcd for $AuC_{53}H_{55}N_2S$ $[M]^+$: *m/z* 948.3746. Elemental analyses: Found (%): C 66.00, H 5.79, N 3.01. Calcd for $C_{53}H_{55}AuN_2S{\cdot}H_2O$: C 65.83, H 5.94, N 2.90.

[Au{4-^{t}BuC^C(4-^{t}BuC$_6$H$_4$)^N$_{(2\text{-thq})}$}(Cbz)] (6)

Orange solid. Yield: 142 mg, 81 %. ^1H NMR (500 MHz, $CDCl_3$, 298 K, relative to Me_4Si, *δ*/ppm): *δ* 8.76−8.74 (d, *J* = 8.8 Hz, 1H, thienoquinolinyl proton), 8.51−8.50 (d, *J* = 5.7 Hz, 1H, thienoquinolinyl proton), 8.27−8.26 (m, 3H, phenyl proton and carbazolyl protons), 8.08−8.06 (d, *J* = 8.0 Hz, 1H, thienoquinolinyl proton), 7.84−7.83 (d, *J* = 5.6 Hz, 1H, thienoquinolinyl proton), 7.68−7.67 (m, 2H, phenyl proton and carbazolyl proton), 7.64−7.58 (m, 5H, phenyl protons and carbazolyl proton), 7.39−7.38 (m, 1H, thienoquinolinyl proton), 7.30−7.28 (d, *J* = 7.9 Hz, 1H, phenyl proton), 7.25−7.21 (m, 2H, carbazolyl protons), 7.11−7.08 (m, 2H, carbazolyl protons), 7.06−7.04 (dd, *J* = 7.9 and 1.9 Hz, 1H, phenyl proton), 7.00−6.95 (m, 1H, thienoquinolinyl proton), 5.73−5.72 (d, *J* = 1.9 Hz, 1H, phenyl proton), 1.43 (s, 9H, −^{t}Bu), 0.72 (s, 9H, −^{t}Bu). $^{13}C\{^1H\}$ NMR (125 MHz, $CDCl_3$, 298 K, relative to Me_4Si, *δ*/ppm): *δ* 167.16, 162.36, 151.72, 151.55, 151.36, 151.03, 150.77, 148.85, 148.36, 144.13, 142.44, 141.90, 138.55, 131.23, 130.81, 130.34, 128.59, 128.14, 128.01, 127.03, 126.04, 126.01, 124.72, 124.67, 124.10, 124.05, 122.93, 122.15, 121.38, 119.76, 116.47, 114.04, 34.69, 34.62. HRMS (Positive ESI): Found *m/z* 886.2621 $[M]^+$. Calcd for $AuC_{49}H_{41}N_2S$ $[M]^+$: *m/z* 886.2650. Elemental analyses: Found (%): C 63.70, H 4.64, N 3.10. Calcd for $C_{49}H_{41}AuN_2S{\cdot}2H_2O$: C 63.77, H 4.91, N 3.04.

Molecular orientation measurements. The gold(III) complexes doped in 3,3′-di(9*H*-carbazol-9-yl)biphenyl (*m*-CBP) thin films were prepared by thermal evaporation on top of precleaned bare silicon substrates. The refractive index and thickness of the films were then determined by the alpha-SE Ellipsometer (J. A. Woollam). Then, 20-nm thick thin films were fabricated on glass substrates that were carefully pre-washed in the same manner as the fused silica substrates. The dipole orientation of the gold(III) complexes was estimated by the Photoluminescence Light Distribution Characteristic Measurement System (C13472-01, Hamamatsu Photonics). All the thin films were freshly prepared to avoid photodegradation of the materials during the measurement. The samples were then attached to a cylindrical lens, with the refractive index of 1.5, via matching oil, and mounted on an automated rotational stage with the film surface precisely positioned at the rotational center of the stage. Photoexcitation of the samples (λ = 365 nm, Power = ~1.5 mW) was performed using a fiber-guided LED output source. The emission from the sample was then collected by a Photonic Multi-Channel Analyzer PMA-12 (C10027-01, Hamamatsu Photonics) through a long-pass filter and a transverse magnetic (TM) mode polarizer. The estimated p_z and order parameter (S) were calculated by the Standard Software (U6039-09, Hamamatsu Photonics), and the angle θ between the normal of a substrate and transition dipole was then calculated by the equation, $S = \frac{3\langle\cos^2\theta\rangle - 1}{2}$, with the bracketed values $\langle \dots \rangle$ indicating an ensemble average of $\langle\cos^2\theta\rangle$.[2] The ratio of the horizontal dipoles to the total dipoles of the emitters (Θ) is obtained by the equation Θ:(1 − Θ) = $\langle\sin^2\theta\rangle$:$\langle\cos^2\theta\rangle$ = h:v.[10,11]

Computational details. All calculations were carried out with the Gaussian 09 suite of programs.[17] By density functional theory (DFT), the ground-state (S_0) geometries of complexes **1**, **3**, **4** and **6** were fully optimized in toluene with the hybrid Perdew, Burke, and Ernzerhof (PBE0) functional,[18–20] in conjunction with the conductor-like polarizable continuum model (CPCM).[21,22] Time-dependent density functional theory[23–25] (TDDFT) calculations at the same level associated with CPCM were then carried out on the optimized S_0 geometries to compute the singlet-singlet transitions in the electronic absorption spectra of **1**, **3**, **4** and **6**. In order to investigate the nature of the emissive states, the geometries of the lowest-lying triplet excited states (T_1) were optimized with the unrestricted UPBE0/CPCM method for **1**, **3**, **4** and **6**. On the basis of the optimized S_0 and T_1 geometries, vibrational frequencies were calculated and all stationary points were verified to be minima on the potential energy surface, as there are no imaginary frequencies observed (NIMAG = 0). In order to gain further insights into the excited states involved in thermally activated delayed fluorescence (TADF) and to compute the ΔE_{ST} value, the geometries of the lowest singlet excited state (S_1) and the T_1 state of **1** were optimized using TDDFT with the PBE0 functional.[18–20] The Cartesian coordinates of the optimized ground- and excited-state geometries are given in **Tables S7−S16**. For all the calculations, the Stuttgart effective core potentials (ECPs) and the associated basis set were used to describe Au[26] with f-type polarization functions (ζ = 1.050),[27] while the 6-31G(d,p) basis set[28–30] was applied for all other atoms. All the DFT and TDDFT calculations were carried out with a pruned (99,590) grid for numerical integration.

OLED fabrication and measurements. OLEDs were fabricated on patterned ITO-coated glass substrates. The substrates were cleaned with Decon 90, rinsed with deionized water, then dried in an oven, and finally treated in an ultraviolet ozone chamber. A 40-nm-thick PEDOT:PSS was spin-coated onto the ITO-coated glass substrates as hole-transporting layer. After that, emissive layer was formed by mixing dendrimers with MCP to prepare a 10 mg cm^{-3} solutions in chloroform and spin-coating onto PEDOT:PSS layer to give 30-nm-thick uniform thin film. After spin-coating, the substrates were mounted onto the sample holder inside the Trovato Vacuum Deposition System and pumped down to high vacuum with base pressure better than 5×10^{-7} Torr. Sequential vapor deposition of a 5-nm-thick 3TPYMB as a hole-blocking layer and a 40-nm-thick TmPyPB as an electron-transporting layer were made onto the PEDOT:PSS layer. Finally, a 1-nm thick LiF and a 150-nm thick Al were deposted as the metal cathode. For the vacuum-deposited OLEDs, sequential thermal evaporation of *α*-NPD (40 nm), TCTA (5 nm), emissive layer, Tm3PyP26PyB (50 nm), LiF (1 nm) and Al (150 nm) were made onto the ITO substrate, in which *α*-NPD, TCTA, and Tm3PyP26PyB were used as hole-transporting, exciton-blocking and electron-transporting layers, respectively. The emissive layer was prepared by co-evaporating Au(III) complex and *m*-CBP as host simultaneously. All the organic materials and metals were put in separate tantalum boats and vapor deposited by resistive heating. All the films were sequentially deposited at a rate of 0.1−0.2 nm s^{-1} without vacuum break. A quartz crystal was equipped in the vacuum deposition system, with which by monitoring the change in resonant frequency due to the additional mass of material deposition onto this crystal, the thickness and deposition rate could be monitored. A shadow mask was used to define the cathode and to make four 0.1 cm^2 devices on each substrate. Current density−voltage−luminance characteristics and EL spectra were measured simultaneously with a programmable Keithley model 2420 power source and a Photoresearch PR-655 spectrometer. The operational lifetime of the vacuum-deposited device was measured by a McScience M6000 OLED lifetime test system.

NMR spectra.

4-^{t}BuC^C(4-^{t}BuC$_6$H$_4$)^N$_{(1\text{-thq})}$

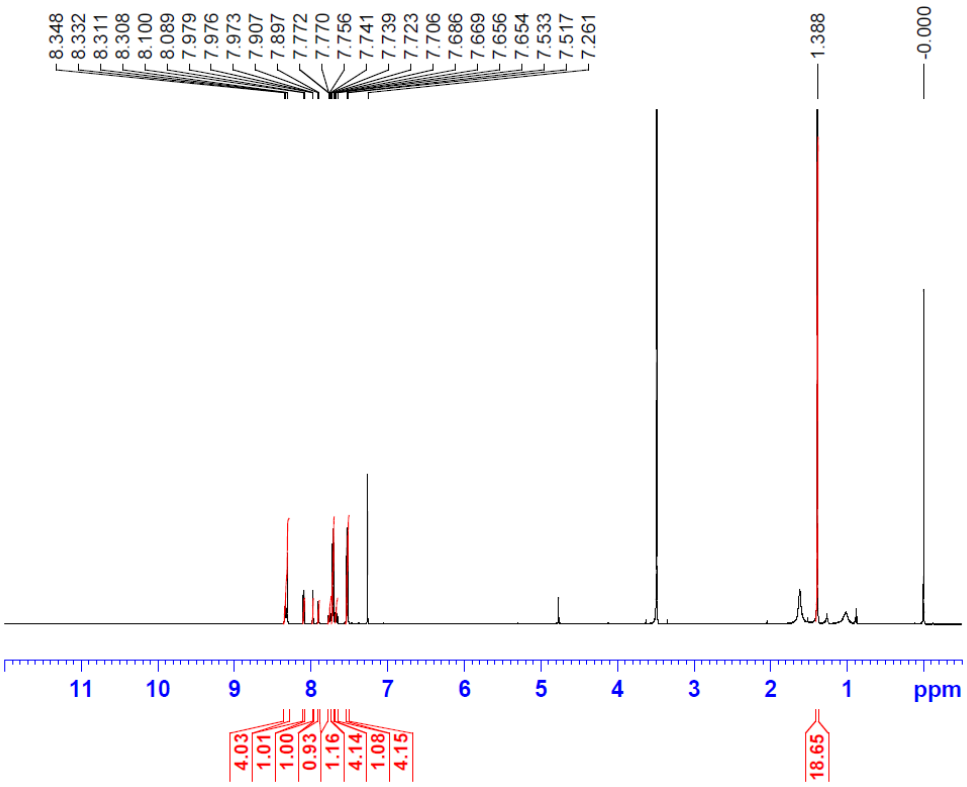

4-^{t}BuC^C(4-^{t}BuC$_6$H$_4$)^N$_{(2\text{-thq})}$

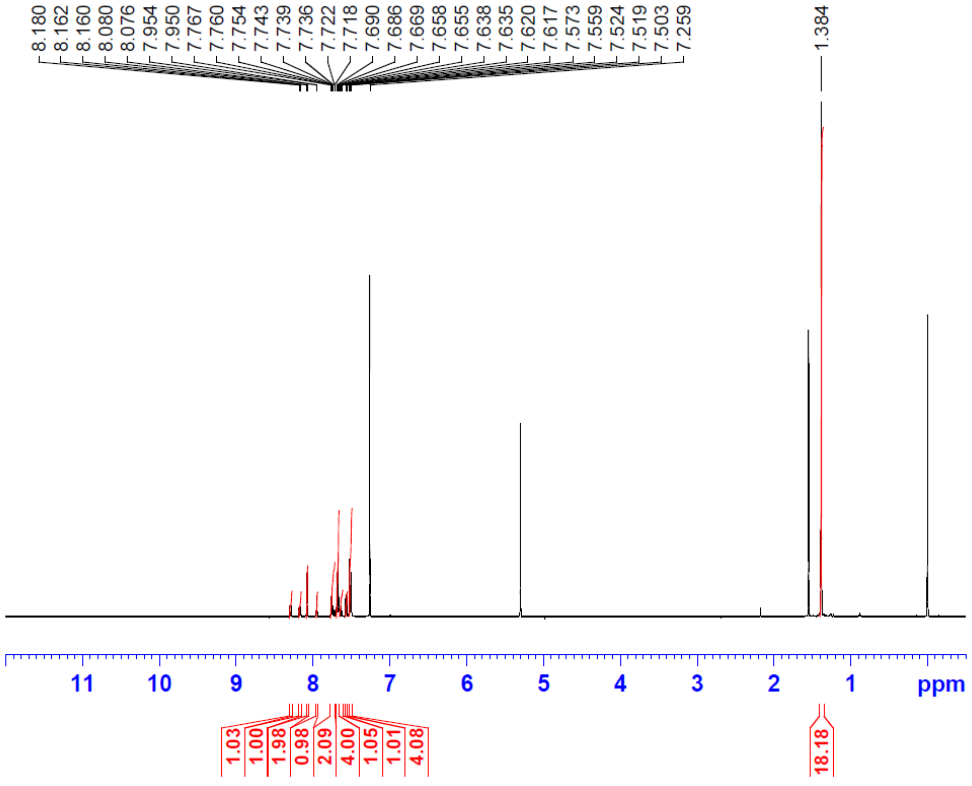

[Au{4-^{t}BuC^C(4-^{t}BuC$_6$H$_4$)^N$_{(1\text{-thpy})}$}Cl]

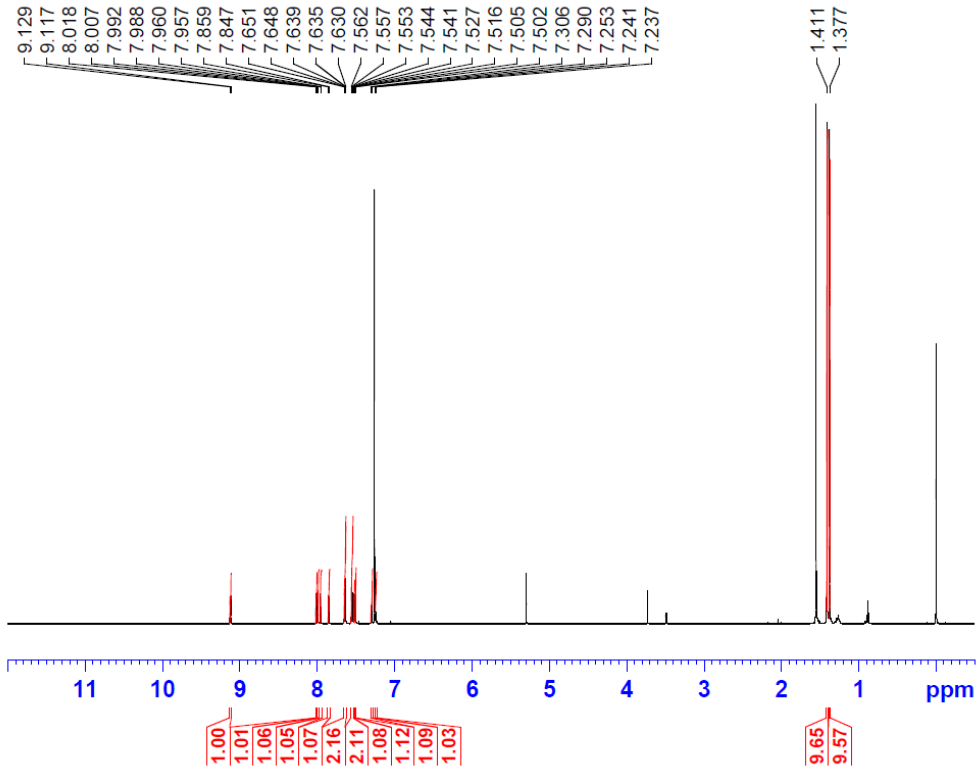

[Au{4-^{t}BuC^C(4-^{t}BuC$_6$H$_4$)^N$_{(2\text{-thpy})}$}Cl]

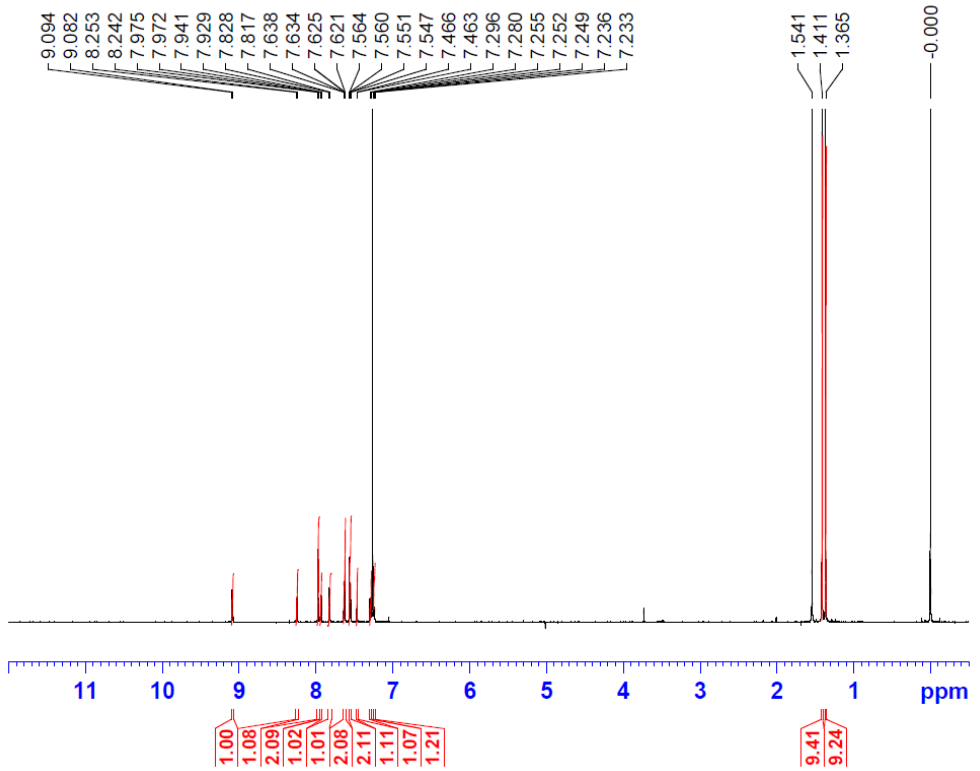

[Au{4-^{t}BuC^C(4-^{t}BuC$_6$H$_4$)^N$_{(1\text{-thq})}$}Cl]

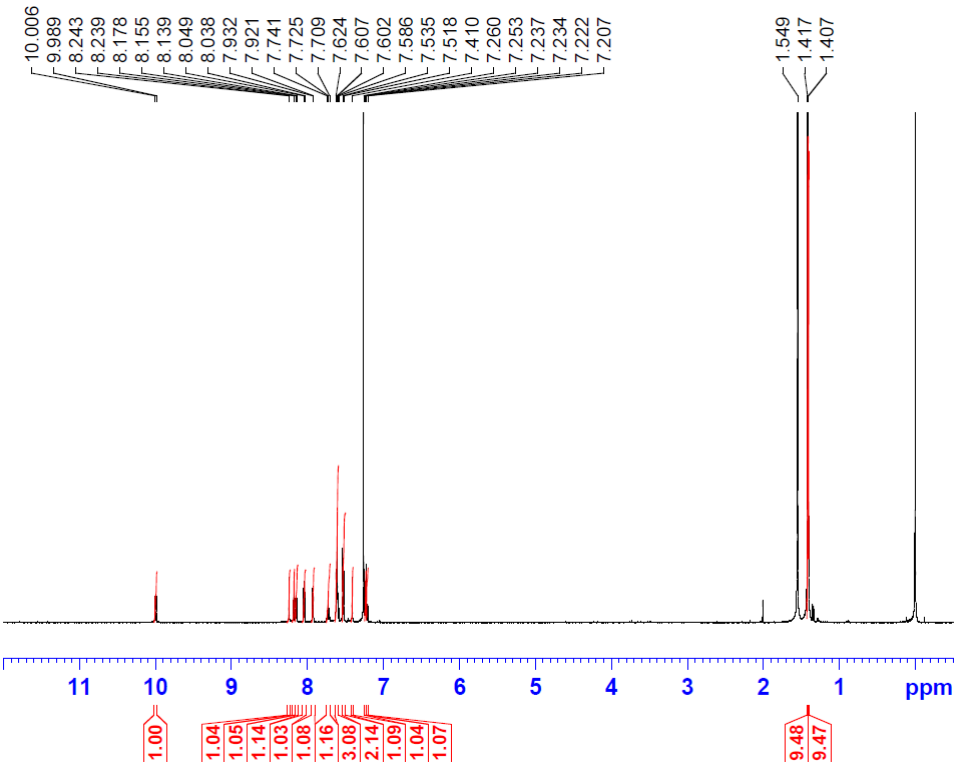

[Au{4-^{t}BuC^C(4-^{t}BuC$_6$H$_4$)^N$_{(2\text{-thq})}$}Cl]

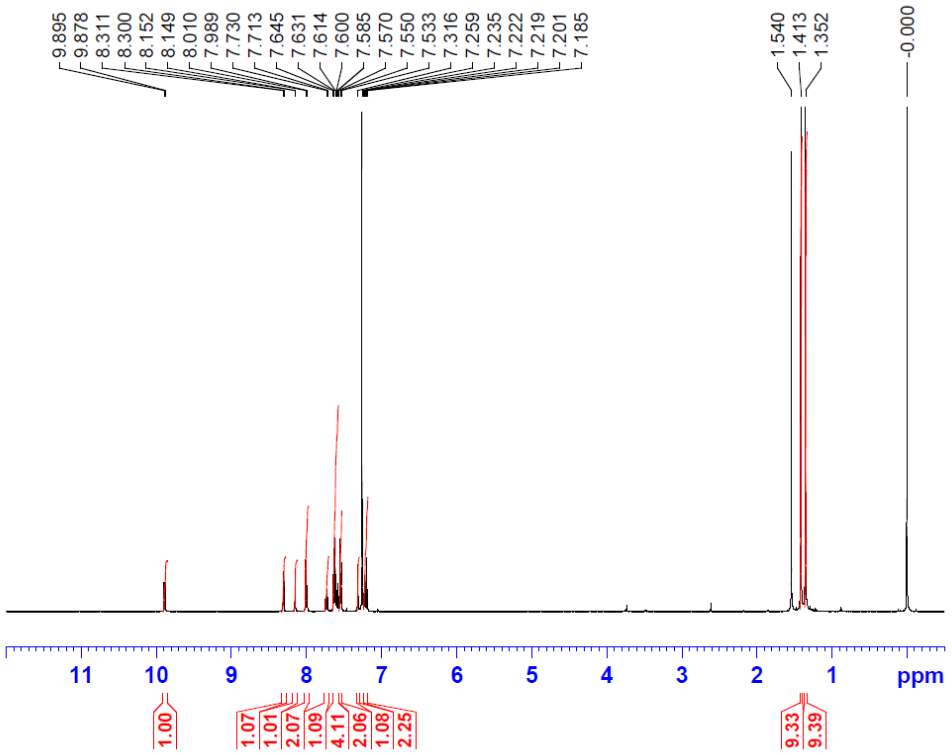

[Au{4-^{t}BuC^C(4-^{t}BuC$_6$H$_4$)^N$_{(1\text{-thpy})}$}(Cbz)] (1)

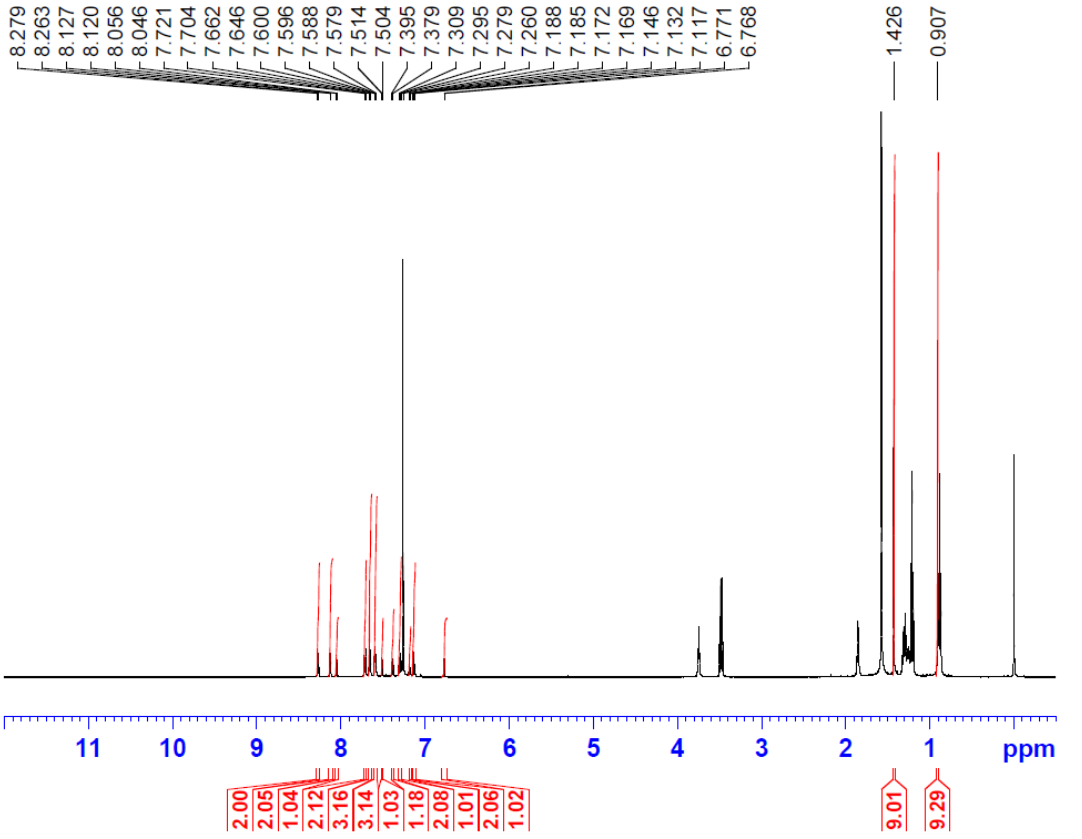

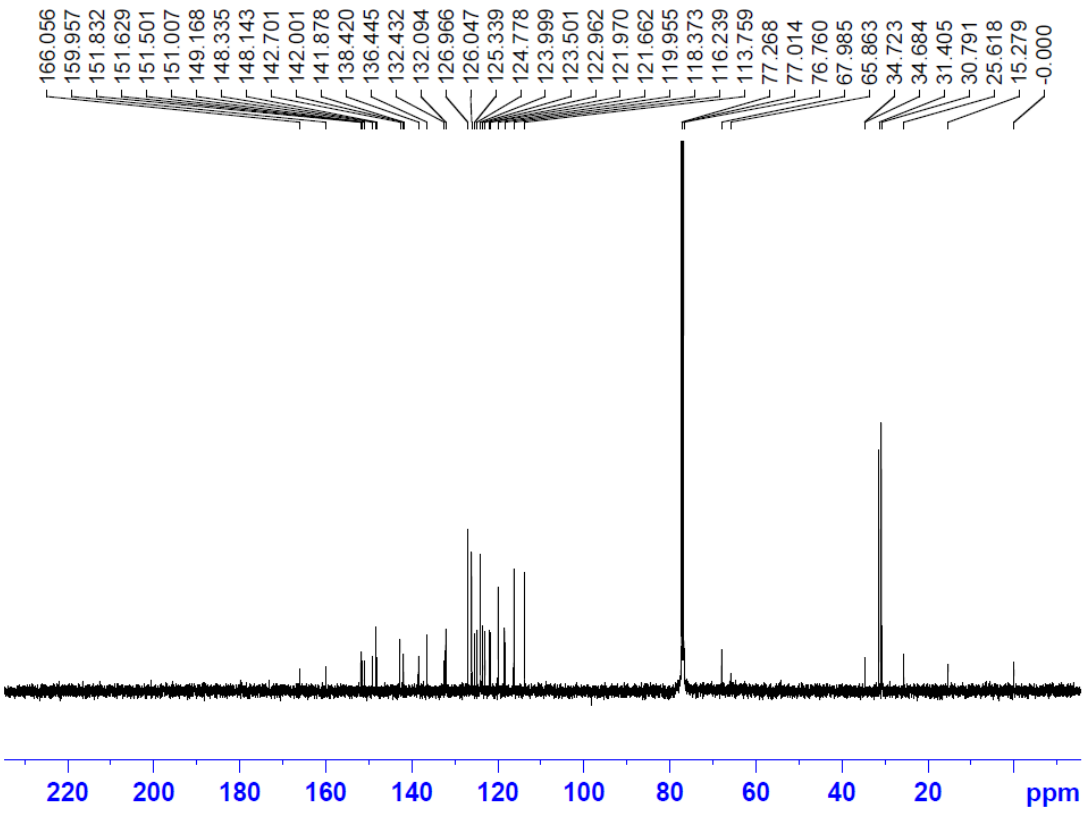

[Au{4-^{t}BuC^C(4-^{t}BuC$_6$H$_4$)^N$_{(1\text{-thpy})}$}(^{t}Bu$_2$Cbz)] (2)

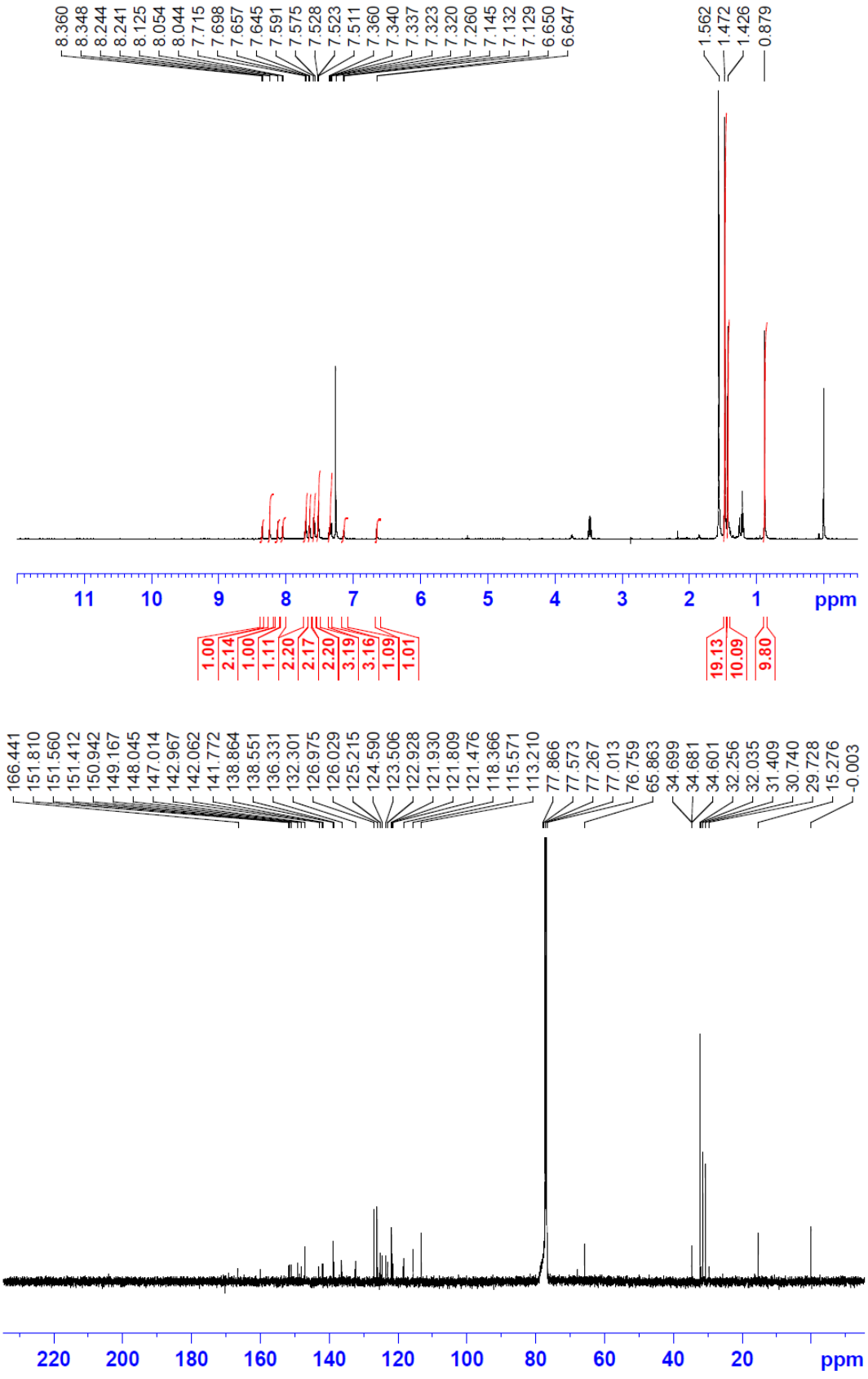

[Au{4-^{t}BuC^C(4-^{t}BuC$_6$H$_4$)^N$_{(1\text{-thq})}$}(Cbz)] (3)

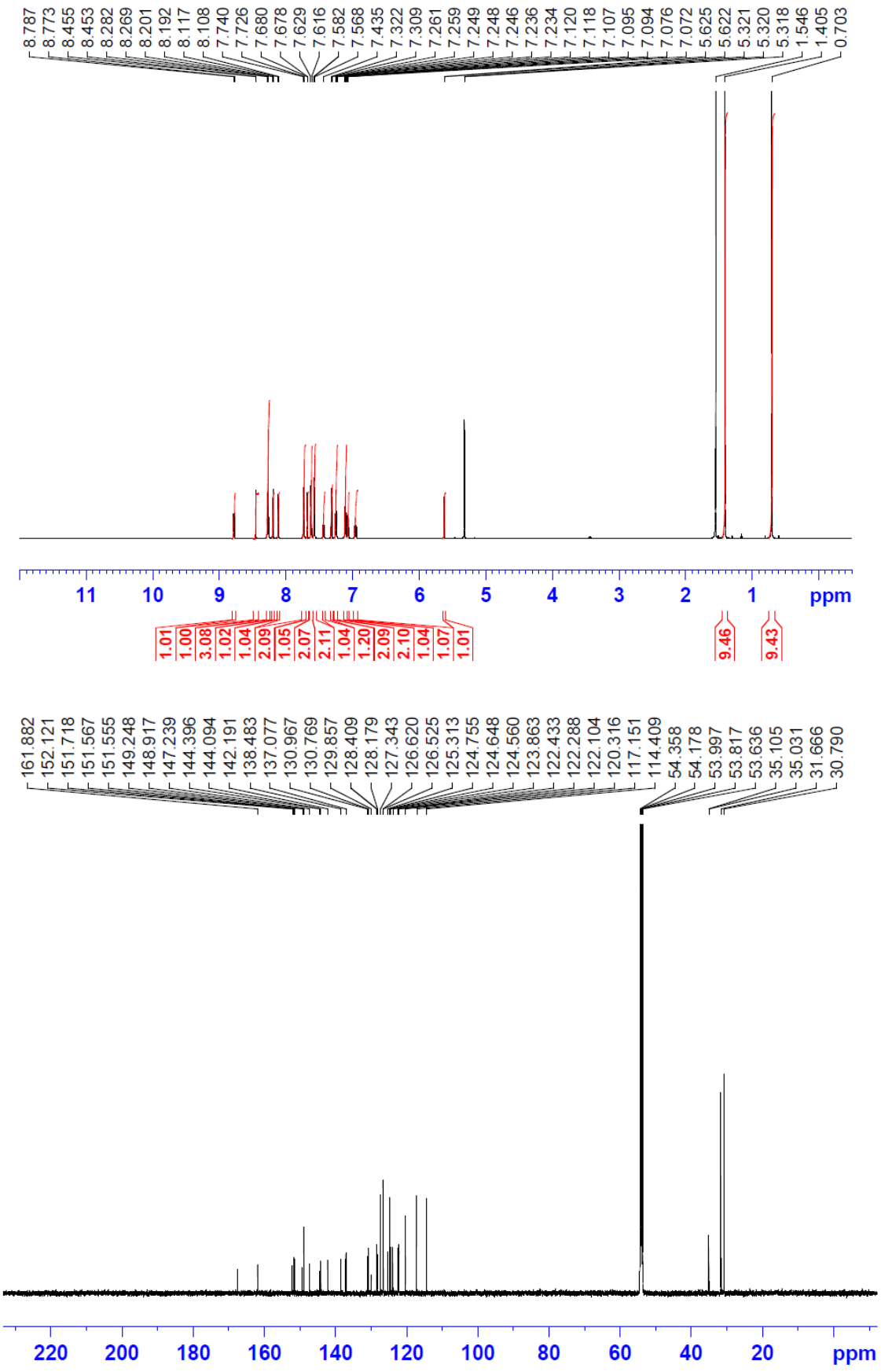

[Au{4-^{t}BuC^C(4-^{t}BuC$_6$H$_4$)^N$_{(2\text{-thpy})}$}(Cbz)] (4)

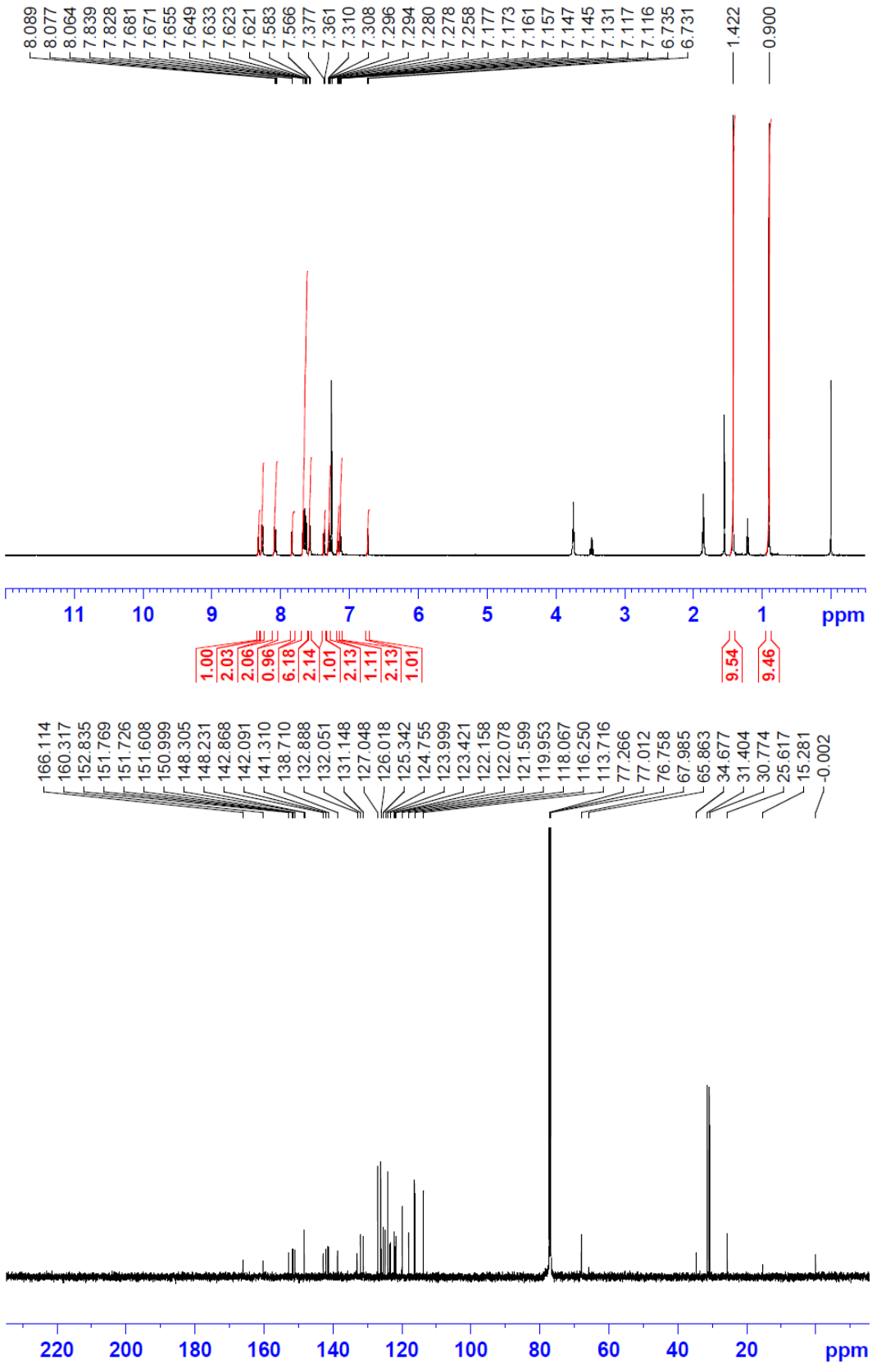

[Au{4-^{t}BuC^C(4-^{t}BuC$_6$H$_4$)^N$_{(2\text{-thpy})}$}(^{t}Bu$_2$Cbz)] (5)

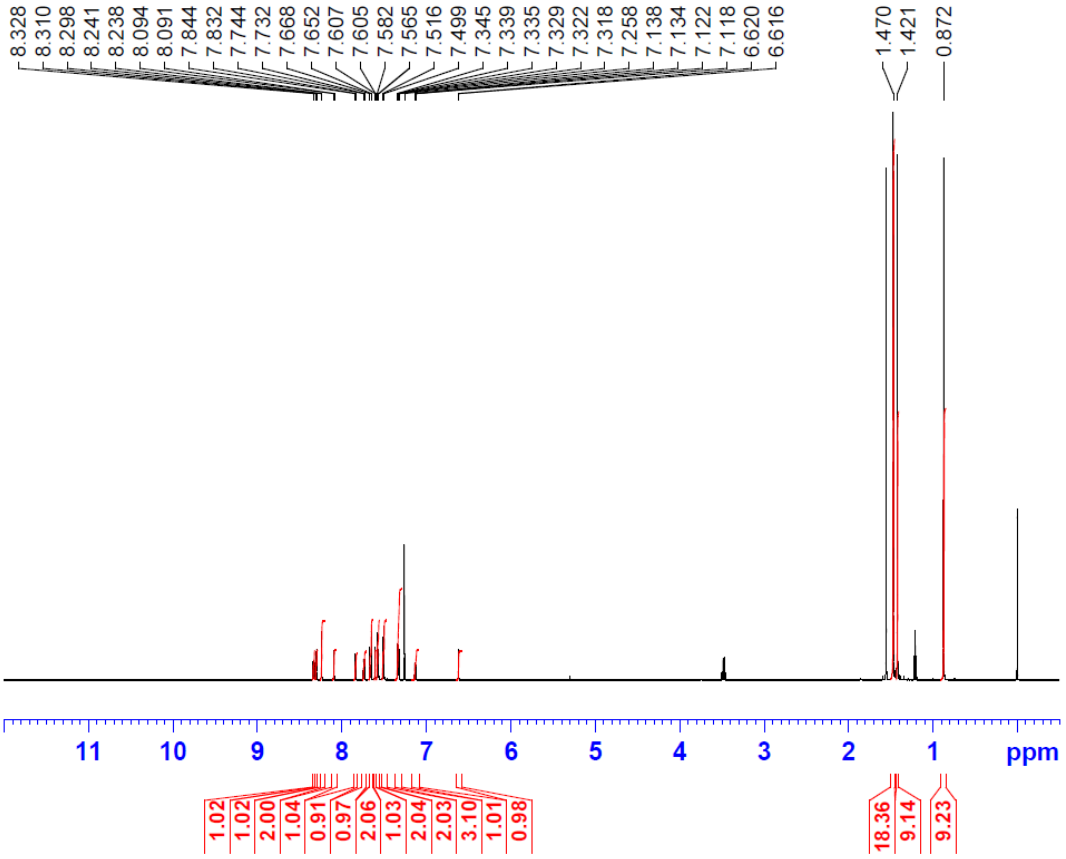

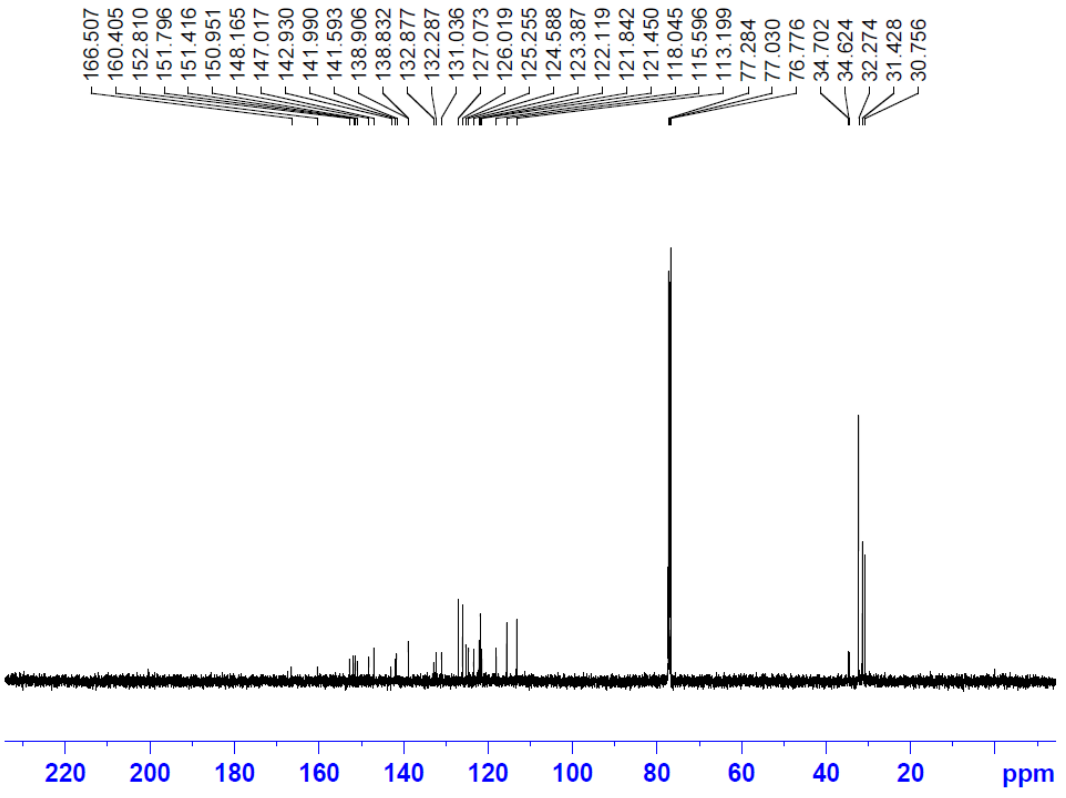

[Au{4-^{t}BuC^C(4-^{t}BuC$_6$H$_4$)^N$_{(2\text{-thq})}$}(Cbz)] (6)

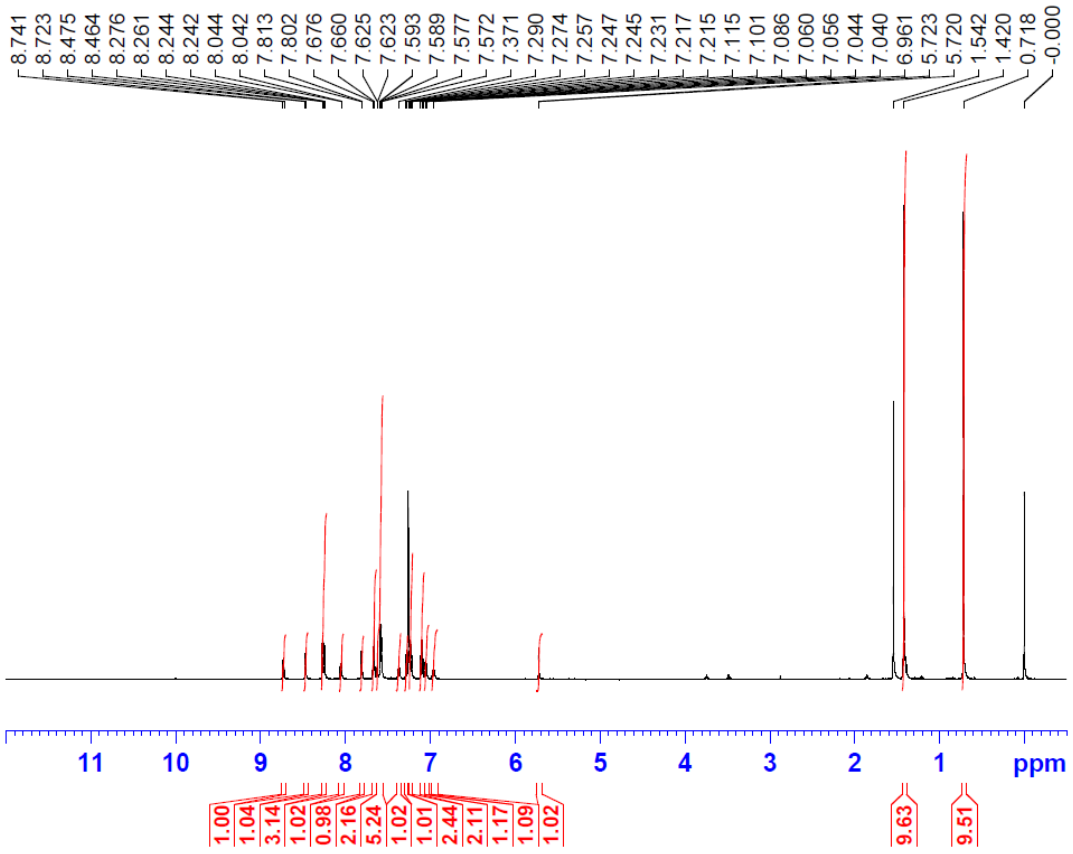

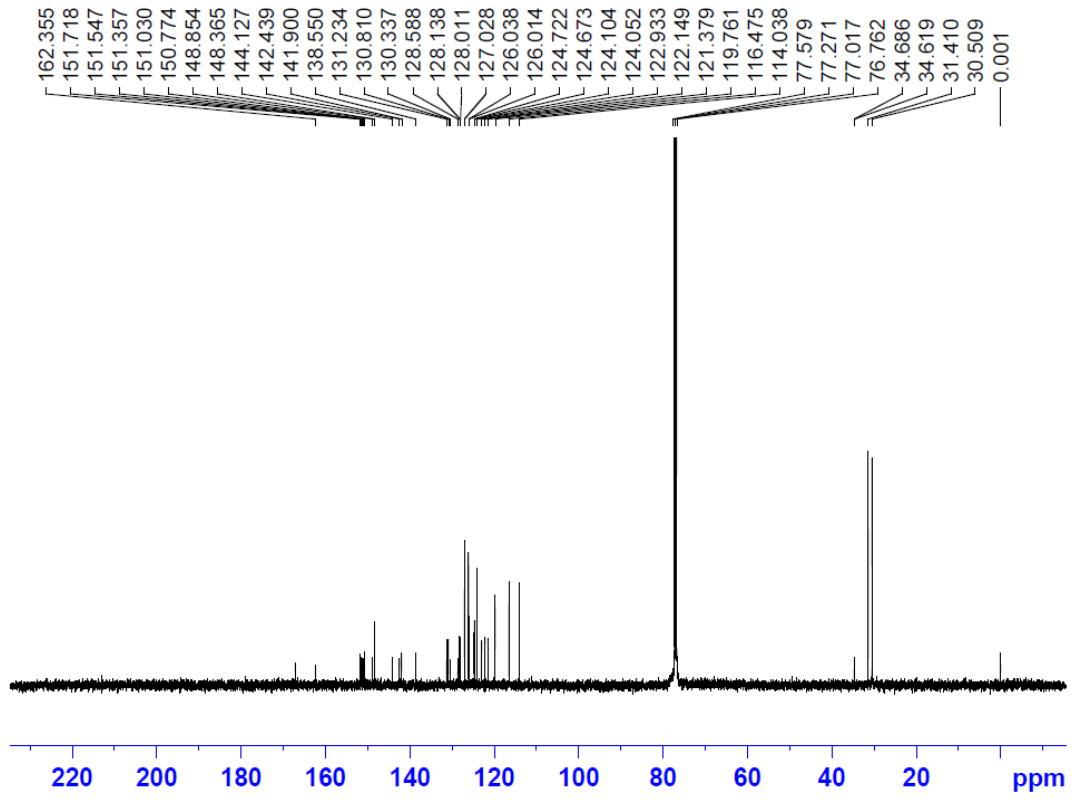

CSI-mass spectra and the corresponding simulated isotope patterns

[Au{4-^{t}BuC^C(4-^{t}BuC$_6$H$_4$)^N$_{(1\text{-thpy})}$}(Cbz)] (1)

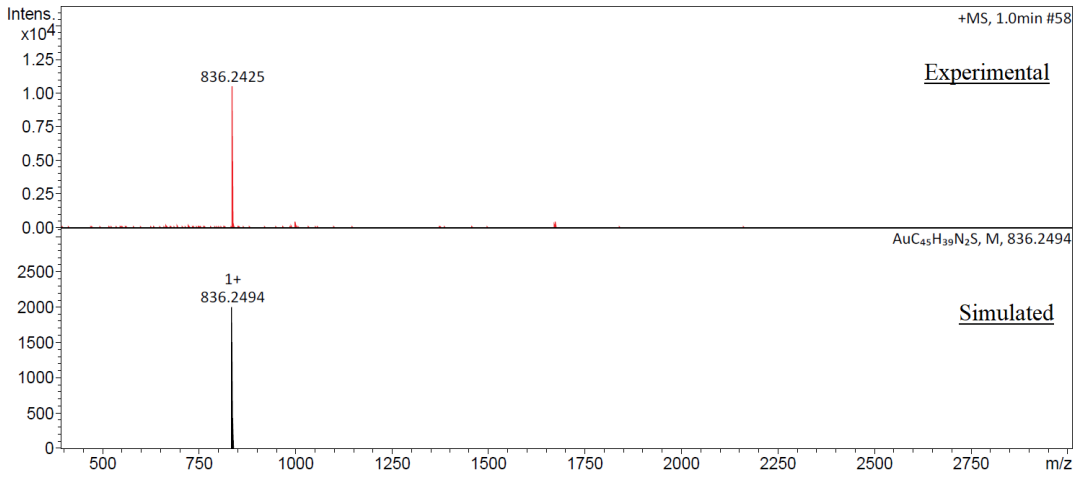

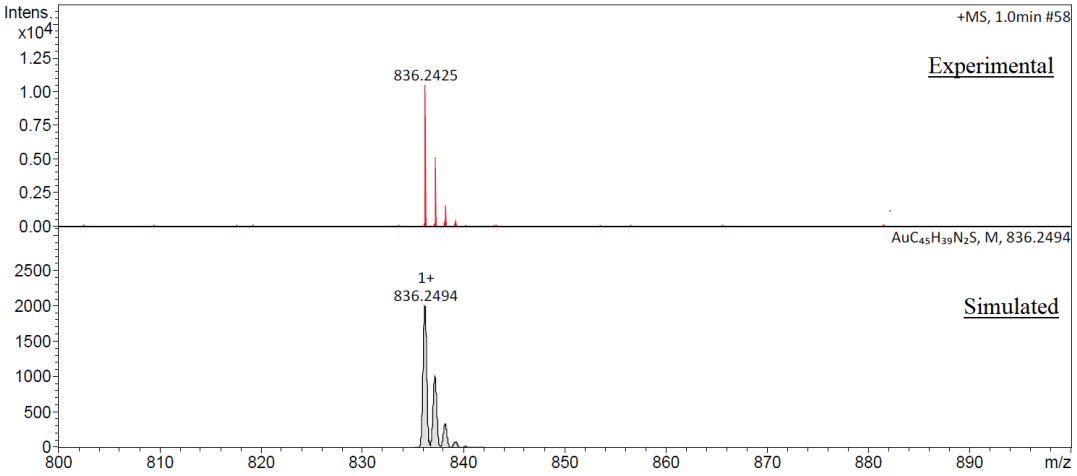

[Au{4-^{t}BuC^C(4-^{t}BuC$_6$H$_4$)^N$_{(2\text{-thpy})}$}(Cbz)] (4)

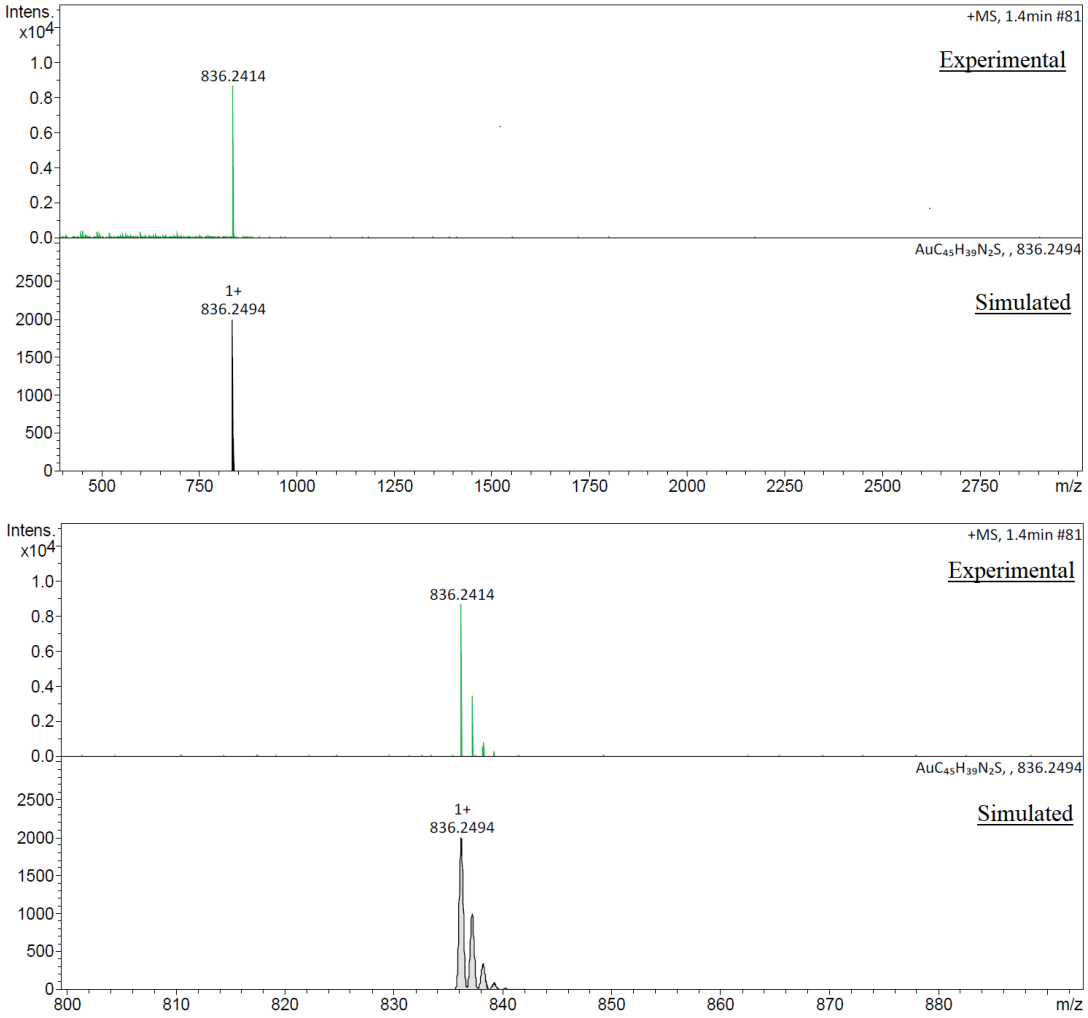

References

1. N. G. Connelly and W. E. Geiger, *Chem. Rev.*, 1996, **96**, 877−910.
2. D. Yokoyama, *J. Mater. Chem.*, 2011, **21**, 19187−19202.
3. T. D. Schmidt, T. Lampe, D. Sylvinson M. R, P. I. Djurovich, M. E. Thompson and W. Brütting, *Phys. Rev. Appl.*, 2017, **8**, 037001.
4. K.-H. Kim and J.-J. Kim, *Adv. Mater.*, 2018, **30**, 1705600.
5. J. Ràfols-Ribé, P.-A. Will, C. Hänisch, M. Gonzalez-Silveira, S. Lenk, J. Rodríguez-Viejo and S. Reineke, *Sci. Adv.*, 2018, **4**, eaar8332.
6. T. Komino, H. Tanaka and C. Adachi, *Chem. Mater.*, 2014, **26**, 3665-3671.
7. K.-H. Kim, S. Lee, C.-K. Moon, S.-Y. Kim, Y.-S. Park, J.-H. Lee, J. Woo Lee, J. Huh, Y. You and J.-J. Kim, *Nat. Commun.*, 2014, **5**, 4769.
8. K.-H. Kim, E. S. Ahn, J.-S. Huh, Y.-H. Kim and J.-J. Kim, *Chem. Mater.*, 2016, **28**, 7505−7510.
9. K.-H. Kim, J.-L. Liao, S. W. Lee, B. Sim, C.-K. Moon, G.-H. Lee, H. J. Kim, Y. Chi and J.-J. Kim, *Adv. Mater.*, 2016, **28**, 2526−2532.
10. T. Marcato and C.-J. Shih, *Helv. Chim. Acta*, 2019, **102**, e1900048.
11. C.-K. Moon, *Molecular Orientation and Emission Characteristics of Ir Complexes and Exciplex in Organic Thin Films*, Springer, 2019.
12. G. A. Crosby and J. N. Demas, *J. Phys. Chem.*, 1971, **75**, 991−1024.
13. R. Kumar, A. Linden and C. Nevado, *Angew. Chem. Int. Ed.*, 2015, **54**, 14287−14290.
14. L.-K. Li, M.-C. Tang, S.-L. Lai, M. Ng, W.-K. Kwok, M.-Y. Chan and V. W.-W. Yam, *Nat. Photon.*, 2019, **13**, 185−191.
15. B. Jiang, X. Ning, S. Gong, N. Jiang, C. Zhong, Z.-H. Lu and C. Yang, *J. Mater. Chem. C*, 2017, **5**, 10220−10224.
16. W.-K. Kwok, M.-C. Tang, S.-L. Lai, W.-L. Cheung, L.-K. Li, M. Ng, M.-Y. Chan and V. W.-W. Yam, *Angew. Chem. Int. Ed.*, 2020, **59**, 9684−9692.
17. M. J. Frisch, G. W. Trucks, H. B. Schlegel, G. E. Scuseria, M. A. Robb, J. R. Cheeseman, G. Scalmani, V. Barone, B. Mennucci, G. A. Petersson, H. Nakatsuji, M. Caricato, X. Li, H. P. Hratchian, A. F. Izmaylov, J. Bloino, G. Zheng, J. L. Sonnenberg, M. Hada, M. Ehara, K. Toyota, R. Fukuda, J. Hasegawa, M. Ishida, T. Nakajima, Y. Honda, O. Kitao, H. Nakai, T. Vreven, J. Montgomery, J. A., J. E. Peralta, F. Ogliaro, M. Bearpark, J. J. Heyd, E. Brothers,

K. N. Kudin, V. N. Staroverov, T. Keith, R. Kobayashi, J. Normand, K. Raghavachari, A. Rendell, J. C. Burant, S. S. Iyengar, J. Tomasi, M. Cossi, N. Rega, J. M. Millam, M. Klene, J. E. Knox, J. B. Cross, V. Bakken, C. Adamo, J. Jaramillo, R. Gomperts, R. E. Stratmann, O. Yazyev, A. J. Austin, R. Cammi, C. Pomelli, J. W. Ochterski, R. L. Martin, K. Morokuma, V. G. Zakrzewski, G. A. Voth, P. Salvador, J. J. Dannenberg, S. Dapprich, A. D. Daniels, O. Farkas, J. B. Foresman, J. V. Ortiz, J. Cioslowski and D. J. Fox, Gaussian, 2013.

18. J. P. Perdew, K. Burke and M. Ernzerhof, *Phys. Rev. Lett.*, 1996, **77**, 3865−3868.
19. J. P. Perdew, K. Burke and M. Ernzerhof, *Phys. Rev. Lett.*, 1997, **78**, 1396−1396.
20. C. Adamo and V. Barone, *J. Chem. Phys.*, 1999, **110**, 6158−6170.
21. V. Barone and M. Cossi, *J. Phys. Chem. A*, 1998, **102**, 1995−2001.
22. M. Cossi, N. Rega, G. Scalmani and V. Barone, *J. Comput. Chem.*, 2003, **24**, 669−681.
23. R. Bauernschmitt and R. Ahlrichs, *Chem. Phys. Lett.*, 1996, **256**, 454−464.
24. M. E. Casida, C. Jamorski, K. C. Casida and D. R. Salahub, *J. Chem. Phys.*, 1998, **108**, 4439−4449.
25. R. E. Stratmann, G. E. Scuseria and M. J. Frisch, *J. Chem. Phys.*, 1998, **109**, 8218−8224.
26. D. Andrae, U. Häußermann, M. Dolg, H. Stoll and H. Preuß, *Theoret. Chim. Acta*, 1990, **77**, 123−141.
27. A. W. Ehlers, M. Böhme, S. Dapprich, A. Gobbi, A. Höllwarth, V. Jonas, K. F. Köhler, R. Stegmann, A. Veldkamp and G. Frenking, *Chem. Phys. Lett.*, 1993, **208**, 111−114.
28. W. J. Hehre, R. Ditchfield and J. A. Pople, *J. Chem. Phys.*, 1972, **56**, 2257−2261.
29. P. C. Hariharan and J. A. Pople, *Theoret. Chim. Acta*, 1973, **28**, 213−222.
30. M. M. Francl, W. J. Pietro, W. J. Hehre, J. S. Binkley, M. S. Gordon, D. J. DeFrees and J. A. Pople, *J. Chem. Phys.*, 1982, **77**, 3654−3665.